Cell Reports
Medicine

Article

Parent-of-origin effects in Alzheimer's liability dissociate neurocognitive and cardiovascular traits in at-risk individuals

Graphical abstract

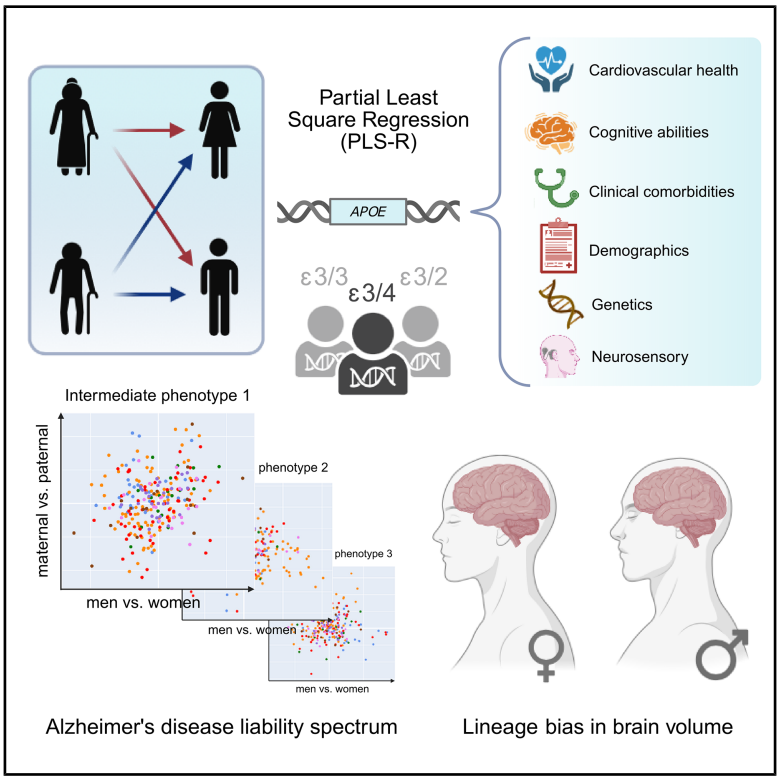

Authors

Chloé Savignac, Frédéric St-Onge, Sylvia Villeneuve, ..., R. Nathan Spreng, Danilo Bzdok, PREVENT-AD Research Group

Correspondence

danilo.bzdok@mcgill.ca

In brief

Savignac et al. show that parent-of-origin effects in Alzheimer's disease extend beyond a classic gender-by-lineage model and instead reflect a complex, context-dependent genetic architecture. They identify and characterize three genetically anchored intermediate phenotypes, which display unique and spatially distributed gender and lineage biases across the brain and phenome.

Highlights

- Genetically anchored parent-of-origin subgroups coexist in Alzheimer's disease
- Three multimodal intermediate phenotypes delineate distinct gender-biased profiles
- Lineage biases in vulnerable brain structures emerge in at-risk individuals

Savignac et al., 2026, Cell Reports Medicine 7, 102943
August 18, 2026
https://doi.org/10.1016/j.xcrm.2026.102943

CellPress

Cell Reports Medicine

CellPress
OPEN ACCESS

Article

Parent-of-origin effects in Alzheimer's liability dissociate neurocognitive and cardiovascular traits in at-risk individuals

Chloé Savignac,[1,2,3] Frédéric St-Onge,[2,4] Sylvia Villeneuve,[4,5,6,7,8] AmanPreet Badhwar,[9,10] Sarah A. Gagliano Taliun,[11,12] Sali Farhan,[6,13] Maiya Geddes,[4,5,6,14,15] Yasser Iturria Medina,[6,7,16] Judes Poirier,[4,5,6,8] R. Nathan Spreng,[4,5,6,7,8,17] Danilo Bzdok,[1,3,7,18,19,*] and PREVENT-AD Research Group

[1]Department of Biomedical Engineering, Faculty of Medicine, McGill University, Montreal, QC, Canada
[2]Integrated Program in Neuroscience, Faculty of Medicine, McGill University, Montreal, QC, Canada
[3]Mila – Quebec Artificial Intelligence Institute, Montreal, QC, Canada
[4]Research Center of the Douglas Mental Health Institute, Montreal, QC, Canada
[5]Centre for Studies in the Prevention of Alzheimer's Disease, Douglas Mental Health Institute, McGill University, Montreal, QC, Canada
[6]Department of Neurology and Neurosurgery, Montreal Neurological Institute (MNI), Faculty of Medicine, McGill University, Montreal, QC, Canada
[7]McConnell Brain Imaging Centre (BIC), MNI, Faculty of Medicine, McGill University, Montreal, QC, Canada
[8]Department of Psychiatry, Faculty of Medicine, McGill University, Montreal, QC, Canada
[9]Department of Pharmacology and Physiology & Institute of Biomedical Engineering, Faculty of Medicine, Université de Montréal, Montreal, QC, Canada
[10]Centre de Recherche de L'Institut Universitaire de Gériatrie de Montréal (CRIUGM), Montreal, QC, Canada
[11]Department of Neurosciences & Department of Medicine, Faculty of Medicine, Université de Montréal, Montreal, QC, Canada
[12]Montreal Heart Institute, Montréal, QC, Canada
[13]Department of Human Genetics, Faculty of Medicine, McGill University, Montreal, QC, Canada
[14]Research Centre for Studies in Aging, Douglas Mental Health Institute, McGill University, Montreal, QC, Canada
[15]McGill University Research Centre for Studies in Aging, Montreal, QC, Canada
[16]Ludmer Centre for Neuroinformatics and Mental Health, McGill University, Montreal, QC, Canada
[17]Department of Psychology, Faculty of Medicine, McGill University, Montreal, QC, Canada
[18]School of Computer Science, McGill University, Montreal, QC, Canada
[19]Lead contact
*Correspondence: danilo.bzdok@mcgill.ca
https://doi.org/10.1016/j.xcrm.2026.102943

SUMMARY

Alzheimer's disease (AD) has a higher prevalence in women than men and is more frequently inherited from mothers than fathers. Yet, while neuroimaging and biomarker studies link maternal family history to stronger AD-related alterations, epidemiological studies suggest that paternal history confers comparable or even greater risk. Here, we leverage the deeply profiled PREVENT-AD cohort to derive three intermediate phenotypes of AD susceptibility. Drawing on nearly 1,000 individual study visits, we quantify how these intermediate phenotypes vary as a function of maternal versus paternal AD lineage. We show that lineage-specific differentiation, including both maternal and paternal biases, is reflected in the brain structure and phenome of adult children of AD patients. Cognitive and cardiovascular risk markers, together with associated genetic variants, show the strongest differentiation along the parental-lineage spectrum of disease susceptibility relative to other correlates of AD burden. Our cross-generational analysis ultimately delineates multidimensional parent-of-origin effects in AD genealogy.

INTRODUCTION

Parental history of sporadic Alzheimer's disease (AD) has been recognized as a key risk factor since the late 1980s.[1] Among AD cases, maternal inheritance is thought to be 1.7–3.6 times more frequent than paternal inheritance.[2] The cumulative risk of developing dementia is ~20%–65% higher for the offspring of AD patients than for individuals without a family history.[3] Sex, in turn, has been considered a non-negligible risk factor for developing AD-type dementia for at least two decades.[3] By 2060, over 13 million Americans are projected to be living with clinical AD, with women alone accounting for 8 million of those cases.[4] The *APOE* ε4 allele, the main genetic risk factor for late-onset AD, increases the risk of AD 4-fold in women aged 65–75 years compared with men, even though the ε4 carriership prevalence is similar across sexes.[5]

Despite the distinct inheritance patterns of maternal and paternal AD risk, the neural and biological mechanisms underlying

Please cite this article in press as: Savignac et al., Parent-of-origin effects in Alzheimer's liability dissociate neurocognitive and cardiovascular traits in at-risk individuals, Cell Reports Medicine (2026), https://doi.org/10.1016/j.xcrm.2026.102943

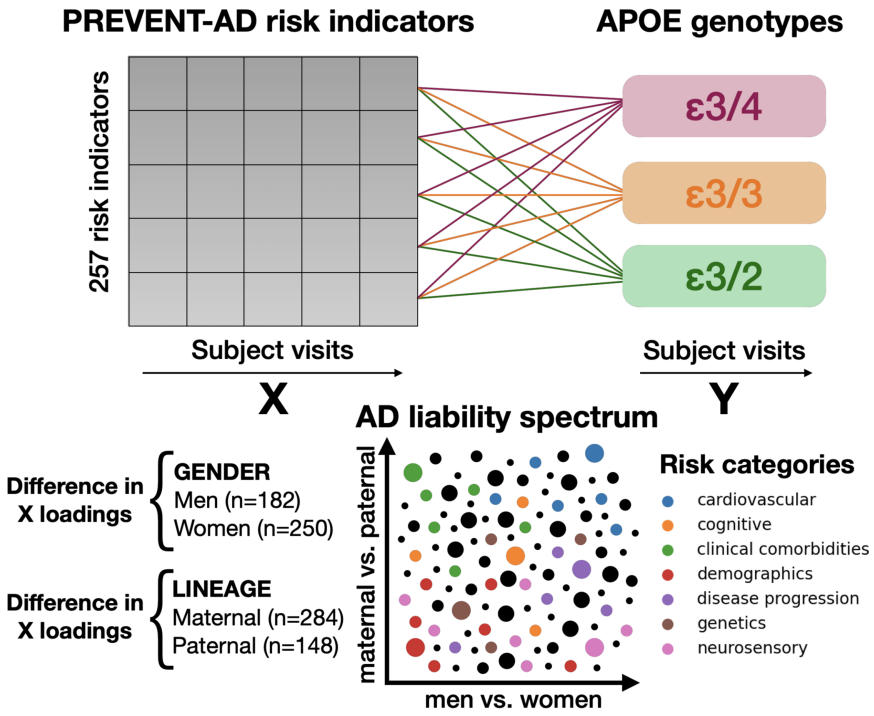

Figure 1. Partitioning variance in PREVENT-AD risk markers by *APOE* genetic risk identifies intermediate phenotypes of AD liability

We built two gender-specific partial least squares regression (PLS-R) models in which variation linked to *APOE* genotypes (e.g., ε3/2, ε3/3, and ε3/4) was used to partition a collection of 257 PREVENT-AD risk indicators spanning 7 broad categories of AD risk factors. Two analogous PLS-R models were built for participants with maternal and paternal history of AD. PLS-R components derived from different subgroups were ordered and aligned using Pearson's correlation (cf. STAR Methods). We subtracted the x-loadings for men and women, as well as for maternal and paternal lineages, to derive category-specific estimates of generational differences in AD risk. This approach allowed us to pinpoint which PREVENT-AD risk indicators exhibited the most significant gender-specific and lineage-specific variation within a given PLS-R component (i.e., intermidiate phenotype [IP]).

these differences remain largely uncharacterized. An early brain imaging study compared maternal vs. paternal AD risk in 11 men and 13 women with a family history.[6] Subsequent work in brain imaging has relied on small clinical samples of at-risk individuals (typically 8–16 subjects[6–10]) that have not allowed disentangling the effects of parental gender across hundreds of brain voxels and clinical markers. The statistical power, arguably too modest, often pushed for case-control investigations in which the genders of the AD at-risk children were not considered. Yet, epidemiological population estimates from more than a million participants—inaccessible to brain imaging assessments at that scale—suggested that men are more vulnerable to developing dementia than women with the same family history.[11]

Rather than being recognized as a risk category in its own right, paternal family history of AD was often treated as a control condition. Against a background of paternal risk, previous studies have established the effects of maternal inheritance on brain volume,[12] mitochondrial activity,[13] glucose metabolism,[8] and cerebral blood flow.[14] A more recent cross-sectional study—with a larger sample size but heterogeneous scanning sites—reported a significant increase in mean β-amyloid (Aβ) on positron emission tomography (PET) in individuals with only a maternal compared with only a paternal history of memory impairment.[15] However, the study's primary analysis—like many before it—relied on a univariate statistical framework that effectively conditioned on offspring sex and parental history instead of examining their effects directly. Perhaps as a consequence of this modeling choice, the authors did not detect a significant interaction between parental history and offspring sex.[15] As a result, the potentially diverging biological and clinical manifestations of maternal and paternal AD risk in at-risk men and women remain uncharted. A direct comparison of the preclinical manifestation of maternal vs. paternal AD risk in men and women—integrating neuroimaging, biological, clinical, and genetic data in a single model—has yet to be undertaken.

Intermediate phenotypes (IPs) offer a powerful strategy to disentangle the contributions of fixed and modifiable risk factors in men and women by enabling the construction of multidimensional scores of preclinical AD manifestations. IPs are measurable biological traits that lie between genetic predispositions and clinical outcomes, capturing subtle, disease-relevant variation across individuals. Adopting IPs can help uncover neural mechanisms underlying complex traits by leveraging risk loci as a link to disease manifestations.[16] This approach is particularly well-suited to complex, oligogenic diseases like AD, where focusing on a select set of genes can improve case-control discrimination. The *APOE* gene alone accounts for over 90% of predictive accuracy in late-onset AD genetic risk[17] and tracks AD-specific brain biomarkers (e.g., hippocampal volume, amyloid burden, and cortical thickness) more robustly than the full polygenic risk score.[18] By adopting a multivariate IP modeling framework, we aimed to partition the variance in *APOE* genetic risk as it relates to the preclinical manifestation of AD in a prospective cohort of adult offspring of AD patients. Our analysis integrates seven broad categories of AD risk factors—cardiovascular health, cognition, clinical comorbidities, demographics, disease progression, genetics, and neurosensory assessments—*in a single model* offering a multidimensional view essential for precision medicine.

RESULTS

Genetically anchored IPs display gender and lineage biases across the phenome

As the backbone of our analysis workflow, we extracted IPs that capture different facets of AD familial risk by being distinctly associated with *APOE* ε3/2, ε3/3, and ε3/4 genotypes (Figure 1). Each derived IP encapsulates a different relationship

Please cite this article in press as: Savignac et al., Parent-of-origin effects in Alzheimer's liability dissociate neurocognitive and cardiovascular traits in at-risk individuals, Cell Reports Medicine (2026), https://doi.org/10.1016/j.xcrm.2026.102943

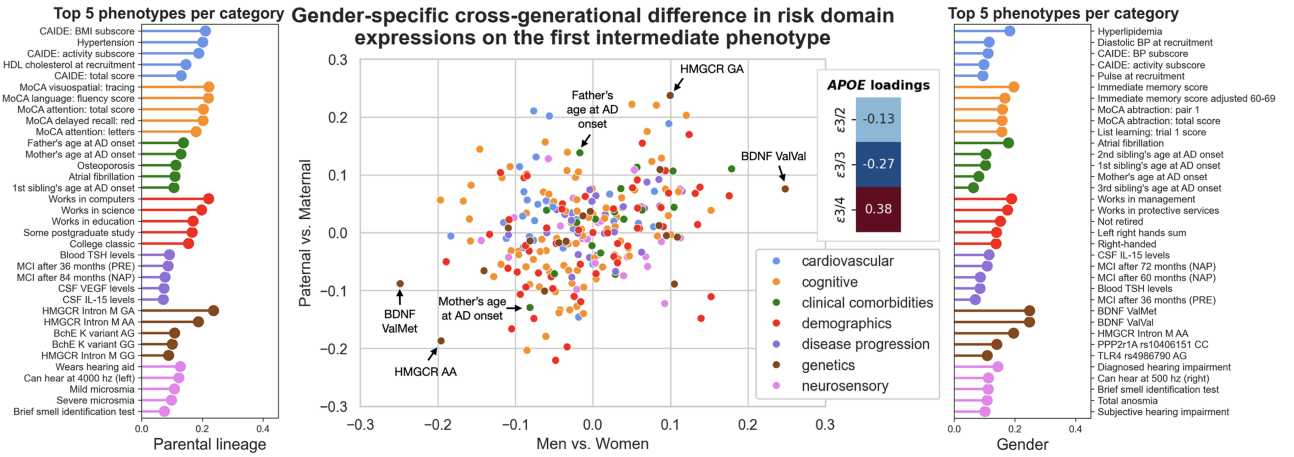

Figure 2. Lineage- and gender-specific biases in genetic markers of memory and lipid metabolism define the leading intermediate phenotype

We built two gender-specific PLS regression (PLS-R) models in which the *APOE* genotypes (e.g., ϵ3/2, ϵ3/3, ϵ3/4) were distinguished based on 257 PREVENT-AD phenotypes (dots in middle scatterplot). Two analogous lineage-specific PLS-R models were built based on subjects with maternal and paternal AD risk. We then subtracted the risk indicators model weights for maternal vs. paternal lineage (*y* axis) and men vs. women (*x* axis). The embedded subplot shows the weights associated with each *APOE* genotype across subjects. The surrounding lollipop plots show the top 5 phenotypes associated with parental lineage (left) and gender (right) (also see accompanying Figure S7). All risk indicators shown in the lollipop plots passed a rigorous bootstrap resampling test and were statistically significant at $\alpha = 0.05$ (Tables S14 and S15). The first IP highlighted cross-generational effects on genetic markers of memory and lipid metabolism. The effect of Val66Met, a missense variant in the gene that codes for BDNF protein, strongly deviated by gender (right lollipop plot). The effect of SNP rs3846662, which is present in intron M of the HMGCR enzyme, was mostly driven by family lineage (left lollipop plot). At the cohort level, the relative contribution of *APOE* ϵ4/3 to the variation in disease manifestation was stronger than for genotypes ϵ3/3 and ϵ3/2 (also see Figure S1). The first IP thus captured cross-generational differences in genetic risk variants associated with proteins involved in memory and lipid metabolism. BchE, butyrylcholinesterase; BDNF, brain-derived neurotrophic factor, BP, blood pressure; CAIDE, cardiovascular risk factors, aging, and incidence of dementia; CSF, cerebrospinal fluid; HDL, high-density lipoprotein; HMCGR, 3-hydroxy-3-methylglutaryl-CoA reductase; IL-15, interleukin-15; IP, intermediate phenotype; MCI, mild cognitive impairment; MoCA, Montreal Cognitive Assessment; PPP2r1A, protein phosphatase 2 scaffold subunit Alpha; TLR4, Toll-like receptor 4; TSH, thyroid-stimulating hormone; and VEGF, vascular endothelial growth factor.

between the three most prevalent *APOE* genotypes and the rich collection of 257 PREVENT-AD risk indicators, selectively emphasizing one genotype over the others (see Figures S1–S3). Each of the three IPs passed a one-sample bootstrap hypothesis test (see Figure S4) and was found to be statistically robust across 1,000 bootstrapped iterations (Pearson's $\rho > 0.75$, p value < 0.0001). The loadings corresponding to the weight of each of the 257 PREVENT-AD risk indicators and three one-hot-encoded *APOE* genotypes on a given IP are shown in Figures S5 and S6, respectively. We assessed how the phenome-wide similarity in AD risk captured by each IP varies as a function of gender and maternal vs. paternal AD familial risk. Our analysis workflow is illustrated in Figure 1.

Our leading IP (explained variance of Pearson's $\rho = 0.76$) highlighted gender differences in genetic markers of memory performance and lipid metabolism. We found that the single-nucleotide polymorphism (SNP) rs6265, also known as Val66Met (Figure 2, right lollipop plot), showed the most substantial gender bias (also see Figures S7B and S7C). Val66Met is a missense variant in the gene that codes for the brain-derived neurotrophic factor (BDNF) protein. BDNF is a neurotrophic factor involved in synaptic plasticity and cognition.[19] The BDNF protein has been associated with several neurological disorders including AD due to its pivotal role in the integrity of hippocampal and neocortical neurons.[20] Over the past two decades, the BDNF Val66Met polymorphism has been one of the most studied genetic variants in neurocognitive brain diseases.[21] Carriers of the Met allele have shown deficits in delayed and immediate recall as well as abnormal hippocampus activation.[22] The Met allele has also been associated with an increased risk of developing AD in women, but not in men.[23,24] We located ValVal homozygotes and ValMet heterozygotes at opposite poles of the gender spectrum of disease variation for the first IP (Figure 2)—consistent with the Val66Met polymorphism's reported gender bias. This association passed a rigorous bootstrap resampling test (see Figure S8). The high magnitude in Cohen's d values, approximately two standard deviations apart (ValVal: Cohen's $d = -2.02$, ValMet: Cohen's $d = 1.92$), suggests that the gender biases identified in *BDNF* are not only statistically significant but also practically relevant. We have thus identified the effects of BDNF Val66Met polymorphism, a key marker of synaptic plasticity, as the principal source of gender bias in AD risk captured by the leading IP.

The first IP also pointed to a genetic variant related to cardiovascular health. We identified SNP rs3846662, located in intron M of the 3-hydroxy-3-methylglutaryl-CoA reductase (HMGCR) gene, as showing strong lineage bias (Figure 2; also see Figures S7E and S7F). *HMGCR* encodes a key enzyme involved in cholesterol synthesis in mammalian cells. In the central nervous system, *HMGCR* is thought to operate in a brain-specific pathway that is separate from, but interrelated with, *APOE*.[25,26] Being homozygous for the A allele (AA) in this intron has been

Please cite this article in press as: Savignac et al., Parent-of-origin effects in Alzheimer's liability dissociate neurocognitive and cardiovascular traits in at-risk individuals, Cell Reports Medicine (2026), https://doi.org/10.1016/j.xcrm.2026.102943

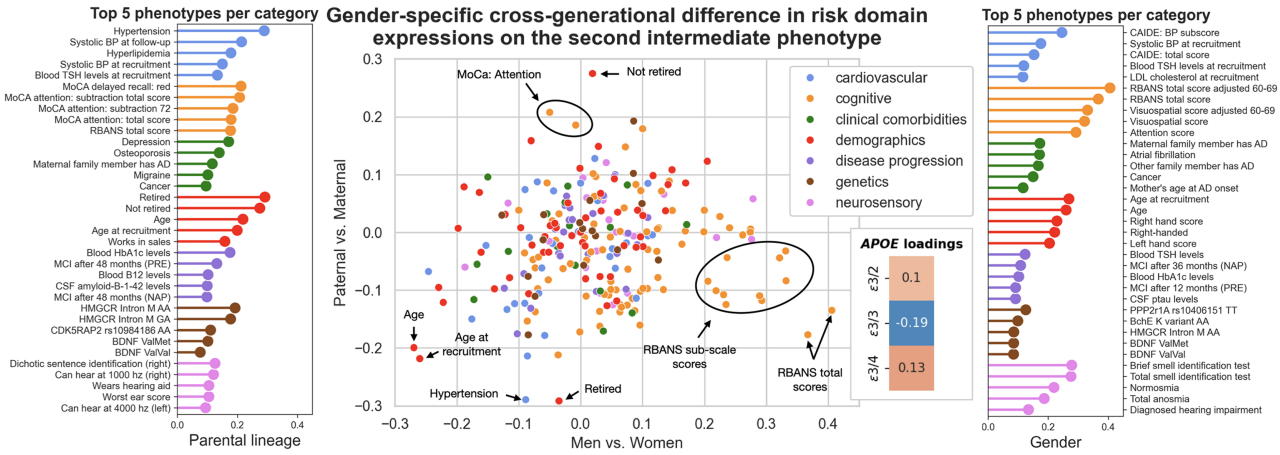

Figure 3. Gender- and lineage-related biases in cognitive risk are the dominant features of the at-risk phenome associated with baseline *APOE* genetic risk

We plotted the gender-specific and lineage-specific effects against each other for the second IP (middle scatterplot). The embedded panel shows the weights associated with each *APOE* genotype across subjects. The surrounding lollipop plots show the top 5 phenotypes associated with parental lineage (left) and gender (right), colored by category of AD risk factors (also see Figure S10). All risk indicators shown in the lollipop plots passed a rigorous bootstrap resampling test and were statistically significant at $\alpha = 0.05$ (Tables S16 and S17). The second IP unveiled notable effects of gender on cognitive indicators that varied in opposite direction to aging-related indicators such as chronological age, hypertension, and retirement status. With regard to *APOE* alleles, this IP distinguished $\epsilon 3$ homozygotes from $\epsilon 4$ and $\epsilon 2$ carriers (also see Figure S2). We thus revealed lineage bases in cognitive risk indicators even relative to the baseline genetic risk for AD. BchE, butyrylcholinesterase; BDNF, brain-derived neurotrophic factor; CAIDE, cardiovascular risk factors, aging, and incidence of dementia; CDK5RAP2, CDK5 regulatory subunit associated protein 2; CSF, cerebrospinal fluid; HbA1c, hemoglobin A1C; HMGCR, 3-hydroxy-3-methylglutaryl-CoA reductase; IP, intermediate phenotype; MCI, mild cognitive impairment; MoCA, Montreal cognitive assessment; PPP2r1A, protein phosphatase 2 scaffold subunit Aalpha; RBANS, Repeatable Battery for Assessment of Neuropsychological Status; TLR4, Toll-like receptor 4; and VEGF, vascular endothelial growth factor.

identified as one of the most important and common protective variants for sporadic AD—second only to *APOE* $\epsilon 2$.[27] The A allele in intron M of the *HMGCR* gene may reduce *APOE* $\epsilon 4$-driven accumulation of amyloid plaques and tangles in the hippocampus and neocortex by modulating cholesterol synthesis in brain cells.[27] Notably, $\epsilon 4$ carriers with the AA genotype show AD conversion rates similar to $\epsilon 4$ non-carriers.[27] Postmortem autopsies of AD patients have revealed increased HMGCR mRNA in the frontal cortex of women, but not men, carrying the AA genotype.[28] Similarly, previous work reported a gender bias among AA carriers, with women showing greater responsiveness to statin therapy than men.[29] We identified lineage bias in *APOE-HMGCR* interaction, with AA homozygotes and GA heterozygotes occupying opposite ends of the disease variation spectrum (Figure 2, scatterplot). This association passed a rigorous bootstrapped resampling test (see Figure S9). *HMGCR* AA, but not GA, also showed a considerable gender bias (Figure 2, right lollipop plot). Consistent with an interplay between *APOE* $\epsilon 4$ and the *HMGCR* A allele, this IP distinguished $\epsilon 4$ carriers from other genotype groups (Figure 2; also see Figure S1). Blood biomarkers further supported the involvement of lipid metabolism, with high-density lipoprotein cholesterol levels at recruitment ranking among the top five cardiovascular indicators whose association with this IP showed parental bias (Figure 2, left lollipop plots). These findings position *HMGCR* AA as a key factor underlying gender- and lineage-specific variation in AD risk, particularly in the context of *APOE* genotype.

The second IP (explained variance of Pearson's $\rho = 0.57$) distinguished *APOE* $\epsilon 3$ homozygotes from $\epsilon 2$ and $\epsilon 4$ carriers (Figure 3). Although *APOE* $\epsilon 3$ homozygotes are often treated as the reference group in AD research—commonly interpreted as representative of typical aging—we observed substantial gender- and lineage-related biases in cognitive risk (see Figure S10). The influence of AD lineage and gender on cognition diverged from that observed for aging-related markers (age, retirement status, and hypertension). Among the most robust findings were group differences in global cognition as measured by the Repeatable Battery for the Assessment of Neuropsychological Status (RBANS), which showed both gender and lineage effects and ranked among the top five markers in each comparison. Visuospatial processing was particularly influenced by gender, whereas working memory—as assessed through the Montreal Cognitive Assessment (MoCA) attention tasks—exhibited pronounced lineage effects (Figure 3, lollipop plots). These findings align with a previous prospective study of middle-aged, asymptomatic offspring of AD patients, which found lower cognitive performance in verbal episodic memory and semantic memory in individuals with parental AD lineage.[30] Nonetheless, in this previous study, no significant differences emerged when directly comparing maternal and paternal groups—likely due to the small number of paternal cases (n = 13). Yet, we revealed clear lineage effects that distinguish cognitive performance on verbal episodic memory tasks as a function of the affected parent's gender. Moreover, we found that the lineage bias in cognitive risk indicators captured by the second IP decreased over time, suggesting that these biases may reflect early or preclinical susceptibility that dampens with the progression of global cognitive decline (see Figure S11). Emergence of these effects in *APOE* $\epsilon 3$ homozygotes, the typical normative aging reference group, reinforces the influence of maternal vs. paternal AD lineage on cognitive vulnerability.

Please cite this article in press as: Savignac et al., Parent-of-origin effects in Alzheimer's liability dissociate neurocognitive and cardiovascular traits in at-risk individuals, Cell Reports Medicine (2026), https://doi.org/10.1016/j.xcrm.2026.102943

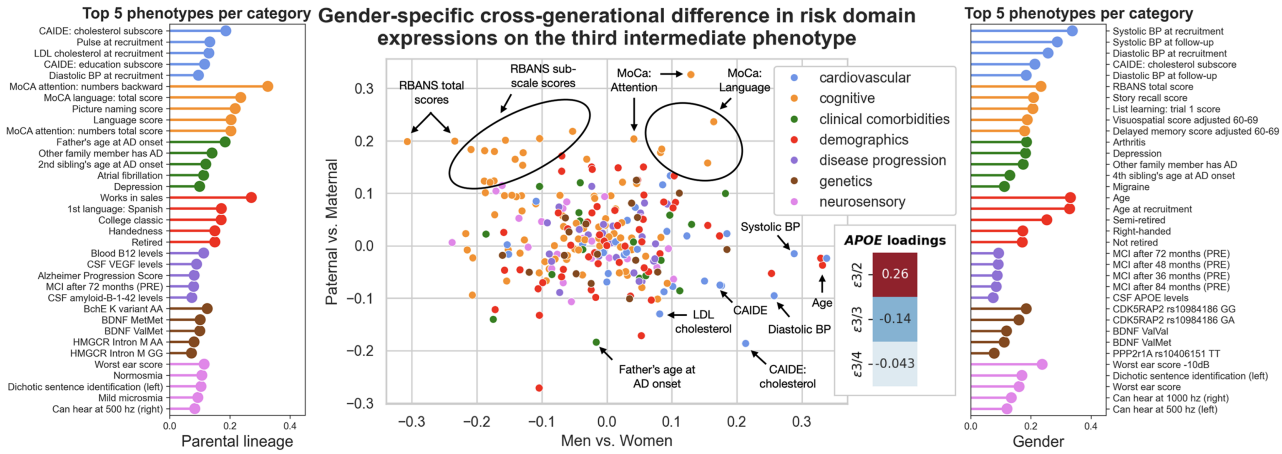

Figure 4. Gender and AD lineage reveal divergent outcomes in memory and cardiovascular health with regard to ϵ2 carriership

We plotted the lineage-specific and gender-specific effects against each other for the third IP (middle scatterplot). The embedded panel shows the weights associated with each *APOE* genotype across subjects. The surrounding lollipop plots show the top 5 phenotypes associated with parental lineage (left) and gender (right), colored by category of AD risk factors (also see Figure S12). All risk indicators shown in the lollipop plots passed a rigorous bootstrap resampling test and were statistically significant at $\alpha = 0.05$ (Tables S18 and S19). The third IP highlighted the combined influence of AD lineage and gender on cognitive abilities and cardiovascular health. The additive cross-generational effects placed cardiovascular (bottom right corner) and cognitive risk indicators (top left corner) in opposite directions on the AD-liability spectrum, with regard to both gender- and lineage-specific variation. Across participants, the relative contribution of *APOE* ϵ3/2 to the variation in disease manifestation captured by the third IP was stronger than for genotypes ϵ3/3 and ϵ3/4 (also see Figure S3). The combined effects of AD lineage and gender, therefore, placed cognitive and cardiovascular risk indicators at antipode on the AD-liability spectrum derived from the third IP. BchE, butyrylcholinesterase; BDNF, brain-derived neurotrophic factor; BP, blood pressure; CAIDE, cardiovascular risk factors, aging, and incidence of dementia; CDK5RAP2, CDK5 regulatory subunit associated protein 2; CSF, cerebrospinal fluid; G-CSF, granulocyte colony-stimulating factor; HMGCR, 3-hydroxy-3-methylglutaryl-CoA reductase; IP, intermediate phenotype; MCI, mild cognitive impairment; MoCA, Montreal Cognitive Assessment; RBANS, Repeatable Battery for Assessment of Neuropsychological status; TLR4, Toll-like receptor 4; and VEGF, vascular endothelial growth factor.

Our third IP (explained variance of Pearson's $\rho = 0.58$) highlighted the simultaneous influence of AD lineage and gender on cardiovascular and cognitive risk indicators (Figure 4). This IP distinguished *APOE* ϵ2 carriers from the other genotype groups (see Figure S3). A first risk group of effects (Figure 4, bottom right corner) highlighted cardiovascular health indicators characteristic of *APOE* ϵ2 carriers (e.g., low-density lipoprotein cholesterol, diastolic and systolic blood pressure) as tied to both gender and AD lineage. At the opposite end of the AD-liability spectrum, we identified a second group of driving effect differences (Figure 4; upper left corner), which encapsulated various dimensions of cognitive performance as measured by the RBANS. Performance on the MoCA varied in the same direction as the RBANS with regard to lineage, but in the opposite direction with regard to gender. Previous work has shown that the ϵ2 allele is typically protective against global cognitive decline and dementia.[31–33] Nonetheless, carrying an ϵ2 allele has been associated with elevated risks for cardio- and neurovascular disorders by previous research groups.[34–39] Mechanistically, the APOE ϵ2 isoform is less efficient in mediating vascular clearance of cholesterol metabolites and triglycerides, which may predispose carriers to hyperlipoproteinemia and related cardiovascular sequelae.[40] The resilience to cognitive decline often observed in *APOE* ϵ2 carriers may partly stem from relatively higher steady-state APOE protein levels in brain regions such as the hippocampus and frontal cortex compared with ϵ4 carriers and ϵ3 homozygotes.[41–44] Hippocampal cell proliferation and survival are strongly modulated by estrogens,[45–47] and the *APOE* promoter contains an estrogen-responsive enhancer element.[48] This regulatory feature may amplify APOE-related effects in women, particularly among ϵ2 carriers. Consistent with this biological framework, the trade-off pattern observed in IP 3 was evident in women (see Figure S12A). Moreover, during the follow-up period, the third IP—differentiating *APOE* ϵ2 carriers from other genotype groups—exhibited a shift toward stronger gender-related biases in cardiovascular risk indicators (see Figure S11). This trajectory is consistent with a trade-off between cardiovascular health and cognitive decline modulated by the ϵ2 allele and amplified by age-related changes in sex hormones.

Maternal vs. paternal AD risk maps onto distinct hippocampal and default network subregions

In a previous UK Biobank (UKB) study, we identified 25 population-level signatures of structural co-variation in hippocampus (HC) and default network (DN) subregions as a function of AD family risk in ~40,000 participants.[39] As an initial exploratory analysis, we examined structural variation across the same 38 HC and 91 DN subregions in PREVENT-AD participants. We used classification models (see STAR Methods) to quantify the extent to which a given subregion reflects maternal vs. paternal AD liability within the full set of HC or DN subregions.

In our analyses of HC subregions, we identified both maternal and paternal lineage effects across genders (Figure 5). We located two robust paternal effects, both lateralized to the left hemisphere, involving the hippocampal molecular layer in men and the presubiculum body in women. Maternal effects were found in the right HC in men and in the left HC in women. The DN showed strong gender biases, with paternal effects again

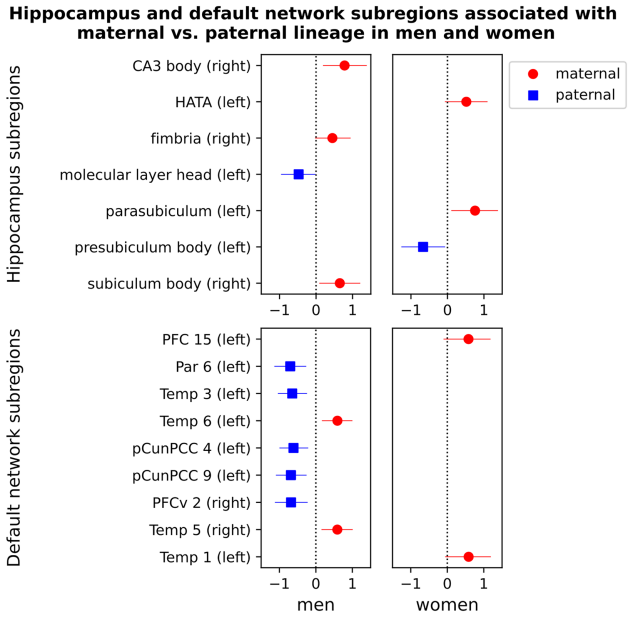

Figure 5. Maternal and paternal AD liabilities are tied to specific HC and DN subregions

We used classification models (maternal = 1, paternal = 0) to assess whether AD lineage differentially targeted brain systems broadly vulnerable in AD: the hippocampus (HC) and default network (DN). We report the coefficients that were statistically different from their respective null distributions 80% of the time (see STAR Methods). In the HC models (top panels), we found maternal biases in the right CA3 body, right fimbria, and right subiculum body in men and in the left HATA and left parasubiculum in women. Paternal biases were identified in the left molecular layer head in men and in the left presubiculum body in women. All significant paternal biases were confined to the left hemisphere. The distribution of maternal and paternal biases in DN subregions showed greater gender biases than for HC subregions. Paternal biases were identified only in men, with the majority located in the left hemisphere (bottom left panel). No overlapping maternal or paternal biases were observed in HC or DN subregions between men and women. HATA, hippocampus-amygdala transition area; pCunPCC, precuneus/posterior cingulate cortex; PFC, prefrontal cortex; PFCv, ventral prefrontal cortex; Par, parietal cortex; and Temp, temporal cortex.

predominant to the left hemisphere, but present only in men. We observed maternal effects in both genders, with bilateral involvement in men and left-hemisphere involvement in women. Emerging PET imaging results from PREVENT-AD suggest that parietal brain regions affected in later stages of AD pathology show stronger lineage biases over time, with individuals with paternal lineage showing faster increase in tau accumulation.[49] We found that gray matter variation in parietal regions of the DN robustly predicted paternal AD lineage in men, whereas no comparable paternal bias was observed in women. In contrast, women showed maternal lineage effects in the left prefrontal and temporal cortices. Overall, these findings highlight gender-specific patterns of cross-generational AD risk, particularly pronounced in neocortical regions of the dominant hemisphere.

The IPs interact with HC-DN signatures in estimating maternal vs. paternal AD risk

We asked whether normative HC-DN co-variation patterns, derived from a representative population, are sensitive to preclinical markers of AD risk in a high-risk cohort. To do so, we projected each PREVENT-AD participant's MRI data onto our previously derived 25 HC-DN co-variation axes, yielding individualized expression scores (see STAR Methods). This approach allowed us to quantify the presence of population-derived structural signatures in a specialized, at-risk cohort and to investigate their relevance to AD-related features. We tested whether incorporating UKB-derived HC-DN co-variation patterns improved the ability of the PREVENT-AD-derived IPs to distinguish maternal from paternal AD lineage in men and women. The classification models incorporated the three IPs, HC/DN co-variation patterns, and their interactions (see STAR Methods).

We found that HC-DN co-variation patterns explained brain variation related to AD family lineage in gender-specific ways (Figure 6). HC-DN co-variation patterns contributed more strongly to the classification of maternal vs. paternal AD risk in men than in women, echoing our earlier diagnostic analysis of subregional gray matter volumes, where we observed a greater number of robust effects in men (Figure 5). In contrast, the IPs were of relatively greater importance in women than in men to differentiate between maternal vs. paternal AD risk. In particular, the first IP showed a robust main effect in women associated with maternal lineage, which persisted across 45 of the 50 women models (Figure 6). In addition, we found robust interaction effects between the first IP and HC and DN co-variation expressions in women, all of which were specific to maternal risk (Figure 6). Conversely, the third IP showed a robust main effect in women associated with paternal lineage. The second IP showed a weaker main effect in distinguishing between maternal and paternal AD risk, with three significant paternal effects found in women and none in men. Nevertheless, it exhibited statistically significant interactions with DN signatures in men and HC signatures in women, involving both maternal and paternal lineage effects (Figure 6). Overall, our findings reveal a gender-specific dissociation in how maternal vs. paternal AD risk manifests. Brain variation contributed more strongly to classifying maternal vs. paternal AD risk in men, whereas we found robust main effects of the first and third IPs in women. These findings suggest that lineage-related effects are more strongly captured by IPs in women, yet more strongly reflected in AD-vulnerable brain structures in men.

Brain-phenotype associations uncover parent-of-origin effects in AD-vulnerable brain structures

We next sought to quantify how maternal vs. paternal AD risk captured by the PREVENT-AD-derived IPs were expressed in AD-vulnerable brain structures. Prior work supports parent-of-origin differences in AD-related biomarkers, although such findings remain heterogeneous.[10,12,15] Our goal was to determine which of the original 38 HC and 91 DN subregions were driving most of the associations between the UKB-derived HC-DN co-variation signatures and the PREVENT-AD-derived IPs. Building on the gender-specific classification models (Figure 6), we mapped the interactions between IPs and HC-DN signatures back onto brain anatomy to identify the regional contributions underlying brain-phenotype associations (cf. STAR Methods). The relative proportion of maternal vs. paternal effects in the DN and HC of men and women probands is shown in Figure S13.

Please cite this article in press as: Savignac et al., Parent-of-origin effects in Alzheimer's liability dissociate neurocognitive and cardiovascular traits in at-risk individuals, Cell Reports Medicine (2026), https://doi.org/10.1016/j.xcrm.2026.102943

CellPress
OPEN ACCESS

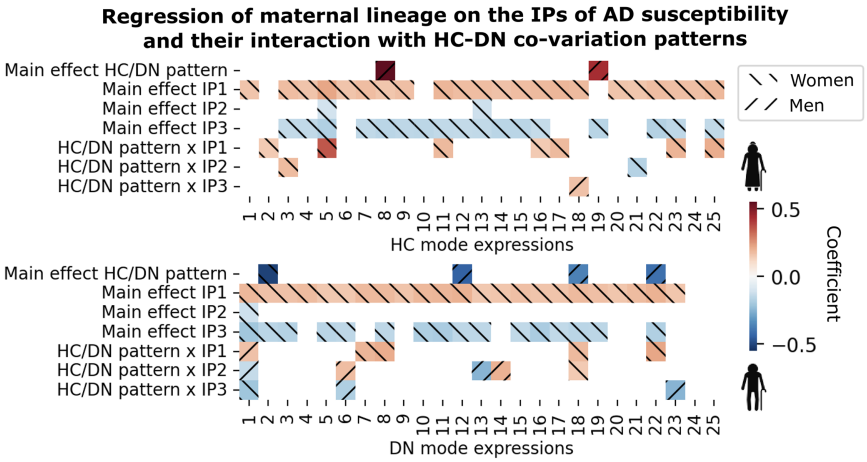

Figure 6. PREVENT-AD intermediate phenotypes interact with HC-DN population co-variation signatures in explaining maternal vs. paternal AD risk

In separated analyses for men and women, we built logistic regression models in which we classified maternal vs. paternal AD lineage (maternal = 1, paternal = 0) as a function of subject-specific expressions of the 3 IPs (computed on the whole PREVENT-AD sample), a given HC or DN co-variation pattern, and the interaction of the given HC or DN co-variation pattern with each of the 3 IPs. Each individual classification model is represented as a distinct column above the heatmaps, on which the HC models (top panel) are separated from the DN models (bottom panel). Effects that were statistically robust in men vs. women at 95% are distinguished with distinct hatching patterns (see legend). Robust main effects of the first and third IPs were found in women and linked to maternal and paternal AD lineage, respectively. In contrast, the relative contribution of the UKB-derived HC-DN co-variation signatures was more important in men than in women, with five robust main effects found in men compared with one in women. Overall, the PREVENT-AD-derived IPs play a relatively more significant role in women than in men in classifying maternal vs. paternal AD risk. Conversely, men exhibited stronger main effects of the UKB-derived HC-DN co-variation signatures, consistent with the men-specific structural associations observed in the diagnostic test. HC, hippocampus; IP, intermediate phenotype; DN, default network; and UKB, UK Biobank.

In IP 1—associated with ε4 carriership—neocortical regions exhibited a spatial dissociation: in women, maternal AD risk was linked to lateral DN subregions, whereas in men, it was associated with medial DN subregions (Figure 7). By contrast, HC subregions associated with maternal and paternal risk were roughly consistent across genders, suggesting shared vulnerability in early tau-prone regions in both men and women, albeit with differences in magnitude. The stronger gender divergence we observed in DN regions mirrors tau replication dynamics in later stages of AD pathology. Indeed, from approximately Braak stage III onward, local replication within a region becomes the dominant driver of tau accumulation, rather than transregional spreading.[50] This shift in dynamics as the AD pathology progresses may contribute to the amplification of subtle age-related gender biases in brain structure. In support of this interpretation, previous work has shown a stronger association between amyloid and tau accumulation in frontotemporal regions related to Braak stages IV and V in women compared with men.[49] Together, these patterns suggest that AD risk tied to ε4 carriership engages shared allocortical structures but diverges across genders in neocortical circuits.

Regarding IP 2, which distinguished *APOE* ε3 homozygotes from other genotypes, nearly all cortical regions exhibited gender-inverted lineage effects. In women, structural variation in all but two of the 91 default network subregions was associated with paternal AD risk, whereas in men, structural variation in all but four subregions was linked to maternal lineage (Figure 7; also see Figure S13). A congruent pattern was observed in the right hippocampal molecular layer (ML), with a paternal bias in women and a maternal bias in men. The ML contains axons branching from pyramidal cells in the CA subfields and subiculum.[51] In the posterior hippocampus, the ML merges into the fimbria of the fornix, which provides the principal hippocampal output to the default network.[52,53] The convergence of maternal and paternal effects in the ML and DN, respectively, highlights the fornix as a key pathway mediating hippocampal-default network communication. This interpretation is supported by prior research identifying fornix fibers as the tract most strongly associated with DN gray matter among 48 anatomical pathways.[54] Altogether, the combined interaction effects of the 25 HC-DN co-variation signatures with the second IP emphasize the role of the ML—and by extension, the fornix—in supporting lineage-specific HC-DN coupling.

The third IP, associated with ε2 carriership, revealed diverging lineage-specific effects in DN regions between genders, yet partially overlapping lineage-specific effects in HC subregions. Although the magnitude was more substantial in men, maternal effects were evident in both genders in the fimbria and CA3 head (Figure 7). We also located corresponding maternal effects in the left ventromedial prefrontal cortex (vmPFC) of both genders—the same hemisphere that showed the most robust positive fimbria weights. This overlap supports the idea of coordinated HC-DN coupling along maternal lines, particularly through the fornix's projections to the vmPFC. This anatomical congruence is biologically plausible, given that the fimbria's projections to the vmPFC via the fornix are considered ipsilateral.[53] Moreover, in men, maternal effects in the fimbria and vmPFC remained detectable despite the presence of strong paternal weights in dorsal DN subregions such as the dmPFC and temporo-parietal junction. Notably, maternal weights in the DN were predominantly located in ventral regions with established anatomical connectivity to the HC. Together, these observations point to a biologically coherent pattern of maternal differentiation across HC and DN subregions—mirroring the known unilateral projections from the HC to ventral DN targets via the fimbria and fornix.

DISCUSSION

We have isolated and characterized a rich collection of maternal and paternal effects in *APOE*-related AD risk from one

Please cite this article in press as: Savignac et al., Parent-of-origin effects in Alzheimer's liability dissociate neurocognitive and cardiovascular traits in at-risk individuals, Cell Reports Medicine (2026), https://doi.org/10.1016/j.xcrm.2026.102943

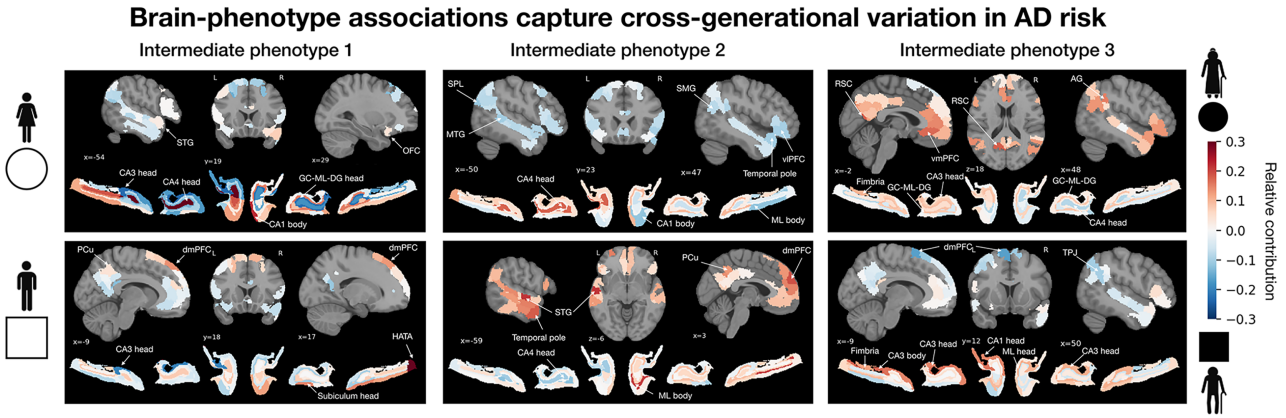

Figure 7. Cross-generational gender biases in AD risk manifest in HC and DN subregions

We plotted the average expression level of the three IPs in each HC and DN subregion (cf. STAR Methods; also see Figure S13 for a summary). Circles indicate women; squares indicate men. Full shading indicates parental lineage. The first IP revealed gender biases in neocortical and allocortical subregions (left panels). Spatial heterogeneity in maternal effects was found in the DN of men and women. Maternal weights were located in lateral structures in women (e.g., left STG and right OFC) when compared with more medial structures in men (e.g., bilateral dmPFC and left PCu). A considerable degree of spatial overlap was found in the HC. In both genders, the left CA3 head was associated with paternal lineage, whereas the left CA4 head, right CA1 body, and right subiculum body and head were associated with maternal lineage. For the second IPs (central panels), nearly the entire DN showed paternal weights in women and maternal weights in men, with ML weights showing the same sign as the DN weights. The third IP revealed mother-to-daughter and father-to-son effects in the DN (right panels). Maternal effects peaked in women in the left RSC, left vmPFC, and right AG, whereas paternal effects were most prominent in men in the left dmPFC and right TPJ. HC overlap was substantial across genders, with maternal weights in the fimbria and CA3 head in both, though effects were stronger in men. Together, these observations suggest a biological pattern of maternal vs. paternal differentiation across HC and DN subregions. AG, angular gyrus; dmPFC, dorsomedial prefrontal cortex; GC-ML-DG, granule cell layer and molecular layer of the dentate gyrus; HATA, hippocampus-amygdala-transition-area; IP, intermmediate phenotype; ML, molecular layer of the subiculum and CA subfields; MTG, middle temporal gyrus; OFC, orbitofrontal cortex; PCu, precuneus; RSC, retrosplenial cortex; SPL, superior parietal lobule; STG, superior temporal gyrus; TPJ, temporo-parietal junction; vlPFC, ventrolateral prefrontal cortex; and vmPFC, ventromedial prefrontal cortex.

generation to the next. This analysis was enabled by a rich homogenously acquired prospective cohort of first-degree relatives of AD patients, with >200 carefully curated phenome markers—the PREVENT-AD initiative. Lineage-specific differentiation in the phenome and brain structure, mirroring known anatomical connections, became apparent in adult children of AD patients. Cognitive and cardiovascular risk markers, along with associated genetic variants, showed the strongest parent-of-origin effects relative to other measures of familial AD burden across *APOE* genetic risk. Several hypotheses have been proposed over the past three decades to explain the differential impact of maternal vs. paternal AD liability.[55] Below, we discuss the core biological mechanisms that may underlie the cross-generational effects captured by our derived IPs. These biological mechanisms, potentially at play in our findings, can be regrouped into three kinds of candidate explanations: mitochondrial alteration, epigenetic imprinting, and chromosome X-mediated heritability.

Mitochondrial DNA is categorically inherited from the mother, making it a biological source of sex bias that can be transmitted over generations.[56] Our first IP highlighted lineage-gender biases for two genetic markers that have previously shown to impact mitochondrial functioning: *HMGCR* and *BDNF* polymorphisms. The Met allele of the *BDNF* gene has been associated with decreased *in vivo* levels of N-acetyl aspartate, a marker of mitochondrial oxidative stress, in the hippocampus of human subjects.[22] Similarly, a high dose of HMGCR inhibitors (statins) has been linked to mitochondrial dysfunction and intracellular oxidative stress in human cell cultures.[57] In its original form, the mitochondrial cascade hypothesis[58,59] holds that mitochondrial dysfunction precedes and potentiates deposition of Aβ aggregates.[59] In more recent years, evidence that Aβ alters mitochondrial functioning has revised the original hypothesis.[60] *In vitro* analyses have suggested that $A\beta_{42}$ peptides could act as a neurotoxin to induce oxidative stress, which impairs mitochondrial functioning.[61] Inversely, cells expressing mitochondrial DNA from AD subjects have shown elevated oxidative stress markers that, in turn, promoted Aβ toxicity and programmed cell death.[62] In a female mouse AD model, embryonic hippocampal neurons showed decreased mitochondrial respiration sustained through the reproductive period and most apparent during reproductive decline.[63] Mitochondrial amyloid load in hippocampal CA1 neurons also increased in this female mouse model.[63] A similar observation has been made in human subjects with maternal AD risk in which elevated cerebrospinal fluid (CSF) levels of F2-isoprostane, a marker of oxidative stress, co-occurred with lower CSF levels of $A\beta_{42/40}$, a marker of amyloid aggregation.[64] Estrogen-signaling pathways could further enhance sex biases in mitochondrial functions, particularly in the hippocampal neurons.[65] In fact, the intact hippocampus has a relatively elevated concentration of steroid hormone receptors compared with the other brain regions.[46] Estradiol may promote mitochondrial respiration, ATP generation, and antioxidant mechanisms.[66] Maternally transmitted mitochondrial DNA could provide a genetic ground by which protective or deleterious haplotypes are passed on from generation to generation.

Please cite this article in press as: Savignac et al., Parent-of-origin effects in Alzheimer's liability dissociate neurocognitive and cardiovascular traits in at-risk individuals, Cell Reports Medicine (2026), https://doi.org/10.1016/j.xcrm.2026.102943

The influence of estrogens throughout females' reproductive age up to senescence could further exacerbate lineage biases in mitochondrial functioning by precipitating Aβ aggregate accumulation and AD pathogenesis. The lineage biases captured by the first IP could thus reflect maternally transmitted genomic effects affecting mitochondrial functioning, potentially amplified by related sex hormone pathways.

Epigenetic regulation provides another plausible mechanism linking the genealogy of AD risk to our findings, with evidence for such effects involving both *HMGCR* and *BDNF*. For *HMGCR*, previous findings suggest that ApoE4-dependent histone modifications alter cholesterol metabolism and memory formation. Specifically, Li and colleagues (2021) showed that astrocytic ApoE regulates neuronal gene expression through modulation of histone acetylation and lipid biosynthesis, including downregulation of *HMGCR*.[67] Notably, ApoE4 particles were less effective in promoting histone acetylation and memory consolidation—suggesting that the epigenetic response to lipid cues is altered in ε4 carriers and may contribute to lineage-specific inheritance of AD risk. These findings align with our observed parent-of-origin biases in *HMGCR* expression and suggest that altered chromatin states may underlie intergenerational transmission of AD vulnerability. A parallel mechanism may also underlie our findings for *BDNF*. Sen and colleagues (2015) demonstrated that ApoE4 promotes nuclear translocation of histone deacetylases, thereby reducing histone acetylation and BDNF expression. In contrast, they found that ApoE3 enhances BDNF transcription via increased acetylation.[68] Interestingly, amyloid-β oligomers were shown to induce similar repressive effects on histone acetylation, suggesting a convergence of ApoE4 and amyloidogenic pathways in downregulating neurotrophins like BDNF.[68] These epigenetic mechanisms provide a plausible substrate for epistatic imprinting, in which parent-of-origin effects at imprinted loci propagate to downstream biallelic genes, producing differential expression depending on which parent contributed the upstream allele. Evidence for such imprinting networks has been demonstrated in mice, with *Hmgcr* in particular identified within an imprinting-by-imprinting epistasis network affecting adipogenesis.[69] Similarly, although imprinting at the Val66Met polymorphism of *BDNF* has not been directly observed, preferential paternal transmission of the valine (G) allele has been reported and associated with increased risk of neurodevelopmental disorders.[70] The same authors previously observed that in the brain frontal cortex of 16 Val/Met heterozygotes, BDNF mRNA from each parental chromosome was expressed at approximately equal levels.[71] This biallelic expression is consistent with *BDNF* acting as a downstream mediator, possibly influenced by upstream parent-of-origin signals, analogous to *HMGCR*. Our lineage biases in AD risk are consistent with a parent-of-origin network that propagates allele-specific epigenetic regulation to *BDNF* and *HMGCR*, ultimately linking parental alleles to AD-relevant phenotypes.

Last, chromosome X-mediated inheritance could represent a contingent source of lineage biases in AD risk. While females generally inherit a chromosome X from both parents, males typically receive a sole chromosome from their mother. Harboring a second X chromosome could represent a biological advantage in conferring resilience toward cognitive deficits in females. Indeed, RNA sequencing of the human dorsolateral prefrontal cortex linked several X chromosome genes to slower cognitive decline in autopsy samples from older females but not males.[72] In contrast, the expression of X genes involved in protein folding was associated with neuropathological tau burden in males but not in females.[72] Animal models of AD pathology corroborated these patterns of X chromosome-mediated vulnerability specific to one sex. Neurons from wild-type mice with the XY genotype are more vulnerable to Aβ-induced toxicity when exposed to recombinant $A\beta_{1-42}$ than those from mice with the XX genotype.[73] The X chromosome likely drove this effect, as similar findings were obtained when comparing neurons from mice with XY and X0 chromosomes to mice with XX and XXY chromosomes.[73] Candidate X genes, such as *Kdm6a*, have emerged from translational work from mice to human as protective against cognitive deficits and Aβ toxicity.[73] An accompanying meta-analysis in humans showed that the male sex (XY genotype) increased the risk for death in AD by 62% when compared with the female sex (XX genotype).[73] Moreover, a genome-wide association study in ~40,000 UKB participants from the imaging cohort identified two X chromosome clusters of brain-gene associations that statistically differ in males and females.[74] The first X chromosome cluster was linked to the metrics of white matter integrity, with peaked effects identified for neurite density in the left superior longitudinal fasciculus.[74] The second cluster highlighted measures of gray vs. white matter intensity contrast in limbic and temporal regions identified as belonging to the DN.[74] It thus seems that harboring a single X chromosome leads to poorer health outcomes, possibly by making the brain more vulnerable to age-related neurotoxicity that eventually precipitates AD pathogenesis. Nonetheless, the frequency of SNP mutations on the X chromosome is reduced by half in male participants. Large-scale multimodal clinical datasets are necessary to support generalizable sex-stratified gene-trait associations.

We disentangled a part of AD risk heterogeneity by identifying genetically anchored IPs varying with offspring and affected parent gender. Our careful filtering of the ever-growing collection of AD risk indicators advocates for therapeutic avenues centered around gender-specific pathways in AD heritability. The different manifestations of maternal and paternal AD risk in men and women are consistent with the co-existence of two distinct disease risk categories rooted in separate biological mechanisms.

Limitations of the study

When interpreting our results, consideration should be given to the scope of the validation strategies employed. While the one-sample bootstrap framework provides a principled and widely used approach to estimate the stability of latent variables,[75–77] it remains confined to the observed dataset and does not constitute external validation. While it provides one of the best available estimates of how sensitive the model results are to fluctuations in the sampled participants, it does not address external generalizability to completely different populations, such as participants with other races or ethnicities. Its primary objective, however, is to quantify the sensitivity of the identified latent components to sampling variability, which it achieves effectively. In this context, it enables us to quantify the robustness of the *APOE*-associated multivariate patterns despite limited subgroup sizes.

To ensure stability of brain signatures,[78] they were first derived in the UKB, the largest available neuroimaging cohort at the time, and then transferred to the target sample. We followed previously established cross-cohort modeling strategies,[76,79] effectively producing out-of-sample estimates. Anchoring these patterns to the IPs, we can assess the reproducibility of the brain-phenotype relationships reported previously[39] in an independent cohort. This provides a complementary form of external validation at the level of associations, even though the underlying neuroanatomical signatures were not independently re-estimated in the smaller cohort.

RESOURCE AVAILABILITY

Lead contact

Further information and requests for resources should be directed to and will be fulfilled by the lead contact, Dr. Danilo Bzdok, (danilo.bzdok@mcgill.ca).

Materials availability

This study did not generate new, unique reagents.

Data and code availability

- Data used in the preparation of this article were obtained from the Pre-symptomatic Evaluation of Novel or Experimental Treatments for Alzheimer's Disease (PREVENT-AD) program, data release 6.0. PREVENT-AD is managed by The Centre for Studies on the Prevention of Alzheimer's Disease (StoP-AD) at the Douglas Mental Health University Institute Research Centre, affiliated with McGill University (https://douglas.research.mcgill.ca/stop-ad-centre). Data management at the StoP-AD Centre is carried out through LORIS (https://loris.ca), which provides the technical infrastructure to manage the acquisition, storing, and conservation of data in order to facilitate data sharing with the greater research community. The PREVENT-AD Open Repository is publicly accessible through the Canadian Open Neuroscience Platform (CONP; ARK ID: https://n2t.net/ark:/70798/d78m93q8n7w4g20mhj) and the institutionally hosted database (https://openpreventad.loris.ca). The Open Repository includes MRI data and basic demographic information. Access requires the creation of an account through https://openpreventad.loris.ca/login/request-account/. Users must agree not to commercialize the dataset or claim intellectual property rights over it; not to attempt to re-identify or re-contact participants, including through linkage with other datasets; to obtain any required ethical approvals; to use the data exclusively for neuroscience research as permitted by participant consent; not to redistribute the data outside the repository; and to comply with monitoring requests and report any breaches of these terms. Eligible academic researchers and physicians may apply for access to the PREVENT-AD Registered Repository, which contains a more comprehensive set of participant data. The Registered Repository is available through CONP (ARK ID: https://n2t.net/ark:/70798/d7j9dvk4777m366kfb) and the institutionally hosted database (https://registeredpreventad.loris.ca). Access requests can be submitted at https://registeredpreventad.loris.ca/login/request-account/. Available data include PET imaging, medical information, genetic data, self-reported questionnaires, neuropsychological assessments, neurosensory evaluations, CSF protein measurements, and magnetoencephalography data. Access is subject to the same commercialization, privacy, ethical oversight, use restriction, confidentiality, and monitoring requirements described above. Following account approval, applicants are contacted by the PREVENT-AD Research Group. Questions regarding access to the Open and Registered Data may be directed to prevenir.alzheimer@douglas.mcgill.ca. The lead contact can help connect you with a member of the StoP-AD Center.
- All individual numerical values underlying the summary data presented in the figures, along with the complete code utilized for their generation, have been made openly accessible on GitHub (https://github.com/chloesavignac/PREVENTAD) and deposited on Zenodo (https://doi.org/10.5281/zenodo.20355121)
- Any additional information required to reanalyze the data reported in this work paper is available from the lead contact upon request.

ACKNOWLEDGMENTS

C.S. received support from fellowships awarded by the Fonds de la Recherche du Québec – Nature et Technologies (FRQNT) and Santé (FRQS) (https://frq.gouv.qc.ca) as well as from the Canadian Institutes of Health Research (CIHR) (https://cihr-irsc.gc.ca). D.B. was supported by the Brain Canada Foundation (https://braincanada.ca) through the Canada Brain Research Fund, with the financial support of Health Canada, National Institutes of Health (https://www.nih.gov) (NIH R01 AG068563A and NIH R01 R01DA053301-01A1), the Canadian Institutes of Health Research (CIHR 438531 and CIHR 470425), the Healthy Brains Healthy Lives Initiative (https://www.mcgill.ca/hbhl/) (Canada First Research Excellence Fund), Google (https://research.google) (Research Award and Teaching Award), and the Canada CIFAR AI Chairs program (https://cifar.ca) (Canada Institute for Advanced Research). J.P. and S.V. were supported by the CIHR, the FRQS, and the J.L. Levesque Foundation (https://fondationjllevesque.org). Data used in the preparation of this article were obtained from the Pre-symptomatic Evaluation of Novel or Experimental Treatments for Alzheimer's Disease (PREVENT-AD) program, data release 6.0. PREVENT-AD was launched in 2011 as a $13.5 million, 7-year public-private partnership using funds provided by McGill University, FRQS, an unrestricted research grant from Pfizer Canada, the J.L. Levesque Foundation, the Douglas Hospital Research Centre and Foundation, the Government of Canada, and the Canada Fund for Innovation. Private sector contributions are facilitated by the Development Office of the McGill University Faculty of Medicine and by the Douglas Hospital Research Center Foundation (http://www.douglas.qc.ca/). Data used in the preparation of this article were obtained from the PREVENT-AD program (https://douglas.research.mcgill.ca/stop-ad-centre), data release 6.0. A complete listing of the PREVENT-AD Research Group can be found in the PREVENT-AD database: https://preventad.loris.ca/acknowledgements/acknowledgements.php?date=2024-04-01. The funders had no involvement in the study's design, data collection, analysis, decision to publish, or manuscript preparation.

AUTHOR CONTRIBUTIONS

C.S. and D.B. conceptualized the study. C.S. analyzed the data and performed the statistical analyses. C.S. worked on data preprocessing and the design of analytic pipelines. D.B. supervised the project. All authors contributed to the writing of the manuscript and interpretation of the results.

DECLARATION OF INTERESTS

D.B. is a shareholder and an advisory board member of MindState Design Labs, USA.

STAR★METHODS

Detailed methods are provided in the online version of this paper and include the following:

- KEY RESOURCES TABLE
- EXPERIMENTAL MODEL AND STUDY PARTICIPANT DETAILS
  - Human participants
- METHOD DETAILS
  - Non-imaging data preprocessing
  - Brain-imaging data preprocessing
- QUANTIFICATION AND STATISTICAL ANALYSIS
  - Intermediate phenotypes of Alzheimer's disease risk
  - Assessment of lineage and gender biases
  - Longitudinal risk analysis
  - Region-wise brain imaging analyses

- Lineage and gender biases in brain signatures
- Back projection of brain-phenotype interaction

SUPPLEMENTAL INFORMATION

Supplementary data related to this article can be found online at https://doi.org/10.1016/j.xcrm.2026.102943.

Received: December 16, 2025
Revised: April 24, 2026
Accepted: June 30, 2026

REFERENCES

1. Breitner, J.C., Silverman, J.M., Mohs, R.C., and Davis, K.L. (1988). Familial aggregation in Alzheimer's disease: Comparison of risk among relatives of early-and late-onset cases, and among male and female relatives in successive generations. Neurology *38*, 207.
2. Duara, R., Lopez-Alberola, R.F., Barker, W.W., Loewenstein, D.A., Zatinsky, M., Eisdorfer, C.E., and Weinberg, G.B. (1993). A comparison of familial and sporadic Alzheimer's disease. Neurology *43*, 1377.
3. Green, R.C., Cupples, L.A., Go, R., Benke, K.S., Edeki, T., Griffith, P.A., Williams, M., Hipps, Y., Graff-Radford, N., Bachman, D., et al. (2002). Risk of dementia among white and African American relatives of patients with Alzheimer disease. JAMA *287*, 329–336.
4. Rajan, K.B., Weuve, J., Barnes, L.L., McAninch, E.A., Wilson, R.S., and Evans, D.A. (2021). Population estimate of people with clinical Alzheimer's disease and mild cognitive impairment in the United States (2020-2060). Alzheimer's Dement. *17*, 1966–1975. https://doi.org/10.1002/alz.12362.
5. Neu, S.C., Pa, J., Kukull, W., Beekly, D., Kuzma, A., Gangadharan, P., Wang, L.S., Romero, K., Arneric, S.P., Redolfi, A., et al. (2017). Apolipoprotein E genotype and sex risk factors for Alzheimer disease: a meta-analysis. JAMA Neurol. *74*, 1178–1189.
6. Mosconi, L., Brys, M., Switalski, R., Mistur, R., Glodzik, L., Pirraglia, E., Tsui, W., De Santi, S., and de Leon, M.J. (2007). Maternal family history of Alzheimer's disease predisposes to reduced brain glucose metabolism. Proc. Natl. Acad. Sci. USA *104*, 19067–19072.
7. Honea, R.A., Swerdlow, R.H., Vidoni, E.D., Goodwin, J., and Burns, J.M. (2010). Reduced gray matter volume in normal adults with a maternal family history of Alzheimer disease. Neurology *74*, 113–120. https://doi.org/10.1212/WNL.0b013e3181c918cb.
8. Mosconi, L., Mistur, R., Switalski, R., Brys, M., Glodzik, L., Rich, K., Pirraglia, E., Tsui, W., De Santi, S., and de Leon, M.J. (2009). Declining brain glucose metabolism in normal individuals with a maternal history of Alzheimer disease. Neurology *72*, 513–520.
9. Honea, R.A., Swerdlow, R.H., Vidoni, E.D., and Burns, J.M. (2011). Progressive regional atrophy in normal adults with a maternal history of Alzheimer disease. Neurology *76*, 822–829. https://doi.org/10.1212/WNL.0b013e31820e7b74.
10. Maye, J.E., Betensky, R.A., Gidicsin, C.M., Locascio, J., Becker, J.A., Pepin, L., Carmasin, J., Rentz, D.M., Marshall, G.A., Blacker, D., et al. (2016). Maternal dementia age at onset in relation to amyloid burden in non-demented elderly offspring. Neurobiol. Aging *40*, 61–67. https://doi.org/10.1016/j.neurobiolaging.2015.12.013.
11. Cannon-Albright, L.A., Foster, N.L., Schliep, K., Farnham, J.M., Teerlink, C.C., Kaddas, H., Tschanz, J., Corcoran, C., and Kauwe, J.S. (2019). Relative risk for Alzheimer disease based on complete family history. Neurology *92*, e1745–e1753.
12. Berti, V., Mosconi, L., Glodzik, L., Li, Y., Murray, J., De Santi, S., Pupi, A., Tsui, W., and De Leon, M.J. (2011). Structural brain changes in normal individuals with a maternal history of Alzheimer's. Neurobiol. Aging *32*, 2325.e17–2325.e26.
13. Mosconi, L., de Leon, M., Murray, J., E, L., Lu, J., Javier, E., McHugh, P., and Swerdlow, R.H. (2011). Reduced mitochondria cytochrome oxidase activity in adult children of mothers with Alzheimer's disease. J. Alzheimers Dis. *27*, 483–490.
14. Okonkwo, O.C., Xu, G., Oh, J.M., Dowling, N.M., Carlsson, C.M., Gallagher, C.L., Birdsill, A.C., Palotti, M., Wharton, W., Hermann, B.P., et al. (2014). Cerebral blood flow is diminished in asymptomatic middle-aged adults with maternal history of Alzheimer's disease. Cerebr. Cortex *24*, 978–988.
15. Seto, M., Hohman, T.J., Mormino, E.C., Papp, K.V., Amariglio, R.E., Rentz, D.M., Johnson, K.A., Schultz, A.P., Sperling, R.A., Buckley, R.F., and Yang, H.S. (2024). Parental History of Memory Impairment and β-Amyloid in Cognitively Unimpaired Older Adults. JAMA Neurol. *81*, 798–804. https://doi.org/10.1001/jamaneurol.2024.1763.
16. Meyer-Lindenberg, A., and Weinberger, D.R. (2006). Intermediate phenotypes and genetic mechanisms of psychiatric disorders. Nat. Rev. Neurosci. *7*, 818–827. https://doi.org/10.1038/nrn1993.
17. Zhang, Q., Sidorenko, J., Couvy-Duchesne, B., Marioni, R.E., Wright, M.J., Goate, A.M., Marcora, E., Huang, K.l., Porter, T., Laws, S.M., et al. (2020). Risk prediction of late-onset Alzheimer's disease implies an oligogenic architecture. Nat. Commun. *11*, 4799.
18. Saadmaan, G., Dalmasso, M.C., Ramirez, A., Hiltunen, M., Kemppainen, N., Lehtisalo, J., Mangialasche, F., Ngandu, T., Rinne, J., Soininen, H., et al. (2024). Alzheimer's disease genetic risk score and neuroimaging in the FINGER lifestyle trial. Alzheimer's Dement. *20*, 4345–4350. https://doi.org/10.1002/alz.13843.
19. Lu, B. (2003). BDNF and activity-dependent synaptic modulation. Learn. Mem. *10*, 86–98.
20. Murer, M.G., Yan, Q., and Raisman-Vozari, R. (2001). Brain-derived neurotrophic factor in the control human brain, and in Alzheimer's disease and Parkinson's disease. Prog. Neurobiol. (1956). *63*, 71–124.
21. Tsai, S.-J. (2018). Critical Issues in BDNF Val66Met Genetic Studies of Neuropsychiatric Disorders. Front. Mol. Neurosci. *11*, 156. https://doi.org/10.3389/fnmol.2018.00156.
22. Egan, M.F., Kojima, M., Callicott, J.H., Goldberg, T.E., Kolachana, B.S., Bertolino, A., Zaitsev, E., Gold, B., Goldman, D., Dean, M., et al. (2003). The BDNF val66met polymorphism affects activity-dependent secretion of BDNF and human memory and hippocampal function. Cell *112*, 257–269.
23. Fukumoto, N., Fujii, T., Combarros, O., Kamboh, M.I., Tsai, S., Matsushita, S., Nacmias, B., Comings, D.E., Arboleda, H., Ingelsson, M., et al. (2010). Sexually dimorphic effect of the Val66Met polymorphism of BDNF on susceptibility to Alzheimer's disease: New data and meta-analysis. American J. of Med. Genetics Pt. B. *153B*, 235–242. https://doi.org/10.1002/ajmg.b.30986.
24. Lin, Y., Cheng, S., Xie, Z., and Zhang, D. (2014). Association of rs6265 and rs2030324 polymorphisms in brain-derived neurotrophic factor gene with Alzheimer's disease: a meta-analysis. PLoS One *9*, e94961.
25. Poirier, J. (2005). Apolipoprotein E, cholesterol transport and synthesis in sporadic Alzheimer's disease. Neurobiol. Aging *26*, 355–361.
26. Yu, C., Youmans, K.L., and LaDu, M.J. (2010). Proposed mechanism for lipoprotein remodelling in the brain. Biochim. Biophys. Acta Mol. Cell Biol. Lipids *1801*, 819–823.
27. Leduc, V., De Beaumont, L., Théroux, L., Dea, D., Aisen, P., Petersen, R.C., the Alzheimer's Disease Neuroimaging Initiative; Dufour, R., and Poirier, J. (2015). HMGCR is a genetic modifier for risk, age of onset and MCI conversion to Alzheimer's disease in a three cohorts study. Mol. Psychiatr. *20*, 867–873. https://doi.org/10.1038/mp.2014.81.
28. Leduc, V., Théroux, L., Dea, D., Dufour, R., and Poirier, J. (2016). Effects of rs3846662 Variants on HMGCR mRNA and Protein Levels and on Markers of Alzheimer's Disease Pathology. J. Mol. Neurosci. *58*, 109–119. https://doi.org/10.1007/s12031-015-0666-7.

29. Leduc, V., Bourque, L., Poirier, J., and Dufour, R. (2016). Role of rs3846662 and HMGCR alternative splicing in statin efficacy and baseline lipid levels in familial hypercholesterolemia. Pharmacogenet. Genom. *26*, 1–11. https://doi.org/10.1097/fpc.0000000000000178.

30. Wilson, K.E., Abulafia, C., Loewenstein, D.A., Vigo, D.E., Sevlever, G., Nemeroff, C.B., Villarreal, M.F., and Guinjoan, S.M. (2018). Individual cognitive and depressive traits associated with maternal versus paternal family history of late-onset Alzheimer's disease: proactive semantic interference versus standard neuropsychological assessments. Pers. Med. Psychiatry *11–12*, 1–6.

31. Corder, E.H., Saunders, A.M., Risch, N.J., Strittmatter, W.J., Schmechel, D.E., Gaskell, P.C., Jr., Rimmler, J.B., Locke, P.A., Conneally, P.M., Schmader, K.E., et al. (1994). Protective effect of apolipoprotein E type 2 allele for late onset Alzheimer disease. Nat. Genet. *7*, 180–184.

32. Farrer, L.A., Cupples, L.A., Haines, J.L., Hyman, B., Kukull, W.A., Mayeux, R., Myers, R.H., Pericak-Vance, M.A., Risch, N., Van Duijn, C.M., et al. (1997). Effects of Age, Sex, and Ethnicity on the Association Between Apolipoprotein E Genotype and Alzheimer Disease: A Meta-analysis. JAMA *278*, 1349–1356. https://doi.org/10.1001/jama.1997.03550160069041.

33. Berlau, D.J., Corrada, M.M., Head, E., and Kawas, C.H. (2009). APOE ε2 is associated with intact cognition but increased Alzheimer pathology in the oldest old. Neurology *72*, 829–834.

34. Nelson, P.T., Pious, N.M., Jicha, G.A., Wilcock, D.M., Fardo, D.W., Estus, S., and Rebeck, G.W. (2013). APOE-ε2 and APOE-ε4 Correlate With Increased Amyloid Accumulation in Cerebral Vasculature. J. Neuropathol. Exp. Neurol. *72*, 708–715. https://doi.org/10.1097/NEN.0b013e31829a25b9.

35. Yu, L., Boyle, P.A., Nag, S., Leurgans, S., Buchman, A.S., Wilson, R.S., Arvanitakis, Z., Farfel, J.M., De Jager, P.L., Bennett, D.A., and Schneider, J.A. (2015). APOE and cerebral amyloid angiopathy in community-dwelling older persons. Neurobiol. Aging *36*, 2946–2953. https://doi.org/10.1016/j.neurobiolaging.2015.08.008.

36. McKay, G.J., Patterson, C.C., Chakravarthy, U., Dasari, S., Klaver, C.C., Vingerling, J.R., Ho, L., de Jong, P.T., Fletcher, A.E., Young, I.S., et al. (2011). Evidence of association of APOE with age-related macular degeneration-a pooled analysis of 15 studies. Hum. Mutat. *32*, 1407–1416.

37. Zhao, N., Liu, C.C., Van Ingelgom, A.J., Linares, C., Kurti, A., Knight, J.A., Heckman, M.G., Diehl, N.N., Shinohara, M., Martens, Y.A., et al. (2018). APOE ε2 is associated with increased tau pathology in primary tauopathy. Nat. Commun. *9*, 4388.

38. Ghebremedhin, E., Schultz, C., Botez, G., Rüb, U., Sassin, I., Braak, E., and Braak, H. (1998). Argyrophilic grain disease is associated with apolipoprotein E ε2 allele. Acta Neuropathol. *96*, 222–224.

39. Savignac, C., Villeneuve, S., Badhwar, A., Saltoun, K., Shafighi, K., Zajner, C., Sharma, V., Gagliano Taliun, S.A., Farhan, S., Poirier, J., and Bzdok, D. (2022). APOE alleles are associated with sex-specific structural differences in brain regions affected in Alzheimer's disease and related dementia. PLoS Biol. *20*, e3001863. https://doi.org/10.1371/journal.pbio.3001863.

40. Mahley, R.W. (2016). Apolipoprotein E: from cardiovascular disease to neurodegenerative disorders. J. Mol. Med. *94*, 739–746. https://doi.org/10.1007/s00109-016-1427-y.

41. Beffert, U., Cohn, J.S., Petit-Turcotte, C., Tremblay, M., Aumont, N., Ramassamy, C., Davignon, J., and Poirier, J. (1999). Apolipoprotein E and β-amyloid levels in the hippocampus and frontal cortex of Alzheimer's disease subjects are disease-related and apolipoprotein E genotype dependent. Brain Res. *843*, 87–94. https://doi.org/10.1016/S0006-8993(99)01894-6.

42. Riddell, D.R., Zhou, H., Atchison, K., Warwick, H.K., Atkinson, P.J., Jefferson, J., Xu, L., Aschmies, S., Kirksey, Y., Hu, Y., et al. (2008). Impact of Apolipoprotein E (ApoE) Polymorphism on Brain ApoE Levels. J. Neurosci. *28*, 11445–11453. https://doi.org/10.1523/jneurosci.1972-08.2008.

43. Ulrich, J.D., Burchett, J.M., Restivo, J.L., Schuler, D.R., Verghese, P.B., Mahan, T.E., Landreth, G.E., Castellano, J.M., Jiang, H., Cirrito, J.R., and Holtzman, D.M. (2013). In vivo measurement of apolipoprotein E from the brain interstitial fluid using microdialysis. Mol. Neurodegener. *8*, 13. https://doi.org/10.1186/1750-1326-8-13.

44. Shinohara, M., Kanekiyo, T., Yang, L., Linthicum, D., Shinohara, M., Fu, Y., Price, L., Frisch-Daiello, J.L., Han, X., Fryer, J.D., and Bu, G. (2016). APOE2 eases cognitive decline during aging: clinical and preclinical evaluations. Ann. Neurol. *79*, 758–774.

45. Galea, L.A.M., and McEwen, B.S. (1999). Sex and seasonal changes in the rate of cell proliferation in the dentate gyrus of adult wild meadow voles. Neuroscience *89*, 955–964.

46. Galea, L.A.M., Wainwright, S.R., Roes, M.M., Duarte-Guterman, P., Chow, C., and Hamson, D.K. (2013). Sex, hormones and neurogenesis in the hippocampus: hormonal modulation of neurogenesis and potential functional implications. J. Neuroendocrinol. *25*, 1039–1061.

47. Tanapat, P., Hastings, N.B., Reeves, A.J., and Gould, E. (1999). Estrogen stimulates a transient increase in the number of new neurons in the dentate gyrus of the adult female rat. J. Neurosci. *19*, 5792–5801.

48. Lambert, J.C., Coyle, N., and Lendon, C. (2004). The allelic modulation of apolipoprotein E expression by oestrogen: potential relevance for Alzheimer's disease. J. Med. Genet. *41*, 104–112.

49. Ourry, V., Fajardo-Valdez, A., Soucy, J.P., Poirier, J., Breitner, J.C., and Villeneuve, S. (2025). Amyloid and tau pathology in cognitively unimpaired individuals with a parental history of Alzheimer disease: role of sex and parent's sex. Neurology *104*, e213507.

50. Meisl, G., Hidari, E., Allinson, K., Rittman, T., DeVos, S.L., Sanchez, J.S., Xu, C.K., Duff, K.E., Johnson, K.A., Rowe, J.B., et al. (2021). In vivo rate-determining steps of tau seed accumulation in Alzheimer's disease. Sci. Adv. *7*, eabh1448.

51. Iglesias, J.E., Augustinack, J.C., Nguyen, K., Player, C.M., Player, A., Wright, M., Roy, N., Frosch, M.P., McKee, A.C., Wald, L.L., et al. (2015). A computational atlas of the hippocampal formation using ex vivo, ultra-high resolution MRI: application to adaptive segmentation of in vivo MRI. Neuroimage *115*, 117–137.

52. Barbas, H., and Blatt, G.J. (1995). Topographically specific hippocampal projections target functionally distinct prefrontal areas in the rhesus monkey. Hippocampus *5*, 511–533. https://doi.org/10.1002/hipo.450050604.

53. Aggleton, J.P., Wright, N.F., Rosene, D.L., and Saunders, R.C. (2015). Complementary Patterns of Direct Amygdala and Hippocampal Projections to the Macaque Prefrontal Cortex. Cerebr. Cortex *25*, 4351–4373. https://doi.org/10.1093/cercor/bhv019.

54. Kernbach, J.M., Yeo, B.T.T., Smallwood, J., Margulies, D.S., Thiebaut de Schotten, M., Walter, H., Sabuncu, M.R., Holmes, A.J., Gramfort, A., Varoquaux, G., et al. (2018). Subspecialization within default mode nodes characterized in 10,000 UK Biobank participants. Proc. Natl. Acad. Sci. USA *115*, 12295–12300.

55. Mattson, M.P. (1997). Mother's legacy: mitochondrial DNA mutations and Alzheimer's disease. Trends in neurosciences (Regular edition) *20*, 373–375.

56. Giles, R.E., Blanc, H., Cann, H.M., and Wallace, D.C. (1980). Maternal Inheritance of Human Mitochondrial DNA, *77* (Proceedings of the National academy of Sciences), pp. 6715–6719.

57. Marcheggiani, F., Cirilli, I., Orlando, P., Silvestri, S., Vogelsang, A., Knott, A., Blatt, T., Weise, J.M., and Tiano, L. (2019). Modulation of Coenzyme Q10 content and oxidative status in human dermal fibroblasts using HMG-CoA reductase inhibitor over a broad range of concentrations. From mitohormesis to mitochondrial dysfunction and accelerated aging. Aging (Albany NY) *11*, 2565–2582.

58. Swerdlow, R.H., and Khan, S.M. (2004). "mitochondrial cascade hypothesis" for sporadic Alzheimer's disease. Med. Hypotheses *63*, 8–20. https://doi.org/10.1016/j.mehy.2003.12.045.

59. Swerdlow, R.H., Burns, J.M., and Khan, S.M. (2010). The Alzheimer's disease mitochondrial cascade hypothesis. J. Alzheimers Dis. *20*, S265–S279.

60. Swerdlow, R.H. (2018). Mitochondria and mitochondrial cascades in Alzheimer's disease. J. Alzheimers Dis. *62*, 1403–1416.

61. Behl, C., Davis, J.B., Lesley, R., and Schubert, D. (1994). Hydrogen peroxide mediates amyloid β protein toxicity. Cell *77*, 817–827. https://doi.org/10.1016/0092-8674(94)90131-7.

62. Cardoso, S.M., Santana, I., Swerdlow, R.H., and Oliveira, C.R. (2004). Mitochondria dysfunction of Alzheimer's disease cybrids enhances Aβ toxicity. J. Neurochem. *89*, 1417–1426. https://doi.org/10.1111/j.1471-4159.2004.02438.x.

63. Yao, J., Irwin, R.W., Zhao, L., Nilsen, J., Hamilton, R.T., and Brinton, R.D. (2009). Mitochondrial bioenergetic deficit precedes Alzheimer's pathology in female mouse model of Alzheimer's disease. Proc. Natl. Acad. Sci. USA *106*, 14670–14675.

64. Mosconi, L., Glodzik, L., Mistur, R., McHugh, P., Rich, K.E., Javier, E., Williams, S., Pirraglia, E., De Santi, S., Mehta, P.D., et al. (2010). Oxidative stress and amyloid-beta pathology in normal individuals with a maternal history of Alzheimer's. Biol. Psychiatry *68*, 913–921.

65. Brinton, R.D. (2008). The healthy cell bias of estrogen action: mitochondrial bioenergetics and neurological implications. Trends Neurosci. *31*, 529–537. https://doi.org/10.1016/j.tins.2008.07.003.

66. Klosinski, L.P., Yao, J., Yin, F., Fonteh, A.N., Harrington, M.G., Christensen, T.A., Trushina, E., and Brinton, R.D. (2015). White matter lipids as a ketogenic fuel supply in aging female brain: implications for Alzheimer's disease. EBioMedicine *2*, 1888–1904.

67. Li, X., Zhang, J., Li, D., He, C., He, K., Xue, T., Wan, L., Zhang, C., and Liu, Q. (2021). Astrocytic ApoE reprograms neuronal cholesterol metabolism and histone-acetylation-mediated memory. Neuron *109*, 957–970.e8. https://doi.org/10.1016/j.neuron.2021.01.005.

68. Sen, A., Nelson, T.J., and Alkon, D.L. (2015). ApoE4 and Aβ Oligomers Reduce BDNF Expression via HDAC Nuclear Translocation. J. Neurosci. *35*, 7538–7551. https://doi.org/10.1523/jneurosci.0260-15.2015.

69. Macias-Velasco, J.F., St Pierre, C.L., Wayhart, J.P., Yin, L., Spears, L., Miranda, M.A., Carson, C., Funai, K., Cheverud, J.M., Semenkovich, C.F., and Lawson, H.A. (2022). Parent-of-origin effects propagate through networks to shape metabolic traits. eLife *11*, e72989.

70. Kent, L., Green, E., Hawi, Z., Kirley, A., Dudbridge, F., Lowe, N., Raybould, R., Langley, K., Bray, N., Fitzgerald, M., et al. (2005). Association of the paternally transmitted copy of common Valine allele of the Val66Met polymorphism of the brain-derived neurotrophic factor (BDNF) gene with susceptibility to ADHD. Mol. Psychiatr. *10*, 939–943. https://doi.org/10.1038/sj.mp.4001696.

71. Bray, N.J., Buckland, P.R., Williams, N.M., Williams, H.J., Norton, N., Owen, M.J., and O'Donovan, M.C. (2003). A haplotype implicated in schizophrenia susceptibility is associated with reduced COMT expression in human brain. Am. J. Hum. Genet. *73*, 152–161.

72. Davis, E.J., Solsberg, C.W., White, C.C., Miñones-Moyano, E., Sirota, M., Chibnik, L., Bennett, D.A., De Jager, P.L., Yokoyama, J.S., and Dubal, D.B. (2021). Sex-Specific Association of the X Chromosome With Cognitive Change and Tau Pathology in Aging and Alzheimer Disease. JAMA Neurol. *78*, 1249–1254. https://doi.org/10.1001/jamaneurol.2021.2806.

73. Davis, E.J., Broestl, L., Abdulai-Saiku, S., Worden, K., Bonham, L.W., Miñones-Moyano, E., Moreno, A.J., Wang, D., Chang, K., Williams, G., et al. (2020). A second X chromosome contributes to resilience in a mouse model of Alzheimer's disease. Sci. Transl. Med. *12*, eaaz5677. https://doi.org/10.1126/scitranslmed.aaz5677.

74. Smith, S.M., Douaud, G., Chen, W., Hanayik, T., Alfaro-Almagro, F., Sharp, K., and Elliott, L.T. (2021). An expanded set of genome-wide association studies of brain imaging phenotypes in UK Biobank. Nat. Neurosci. *24*, 737–745.

75. Efron, B., and Tibshirani, R.J. (1994). An Introduction to the Bootstrap (Chapman and Hall/CRC).

76. Kopal, J., Kumar, K., Saltoun, K., Modenato, C., Moreau, C.A., Martin-Brevet, S., Huguet, G., Jean-Louis, M., Martin, C.O., Saci, Z., et al. (2023). Rare CNVs and phenome-wide profiling highlight brain structural divergence and phenotypical convergence. Nat. Hum. Behav. *7*, 1001–1017.

77. Saltoun, K., Adolphs, R., Paul, L.K., Sharma, V., Diedrichsen, J., Yeo, B.T.T., and Bzdok, D. (2022). Dissociable brain structural asymmetry patterns reveal unique phenome-wide profiles. Nat. Hum. Behav. *7*, 251–268.

78. Helmer, M., Warrington, S., Mohammadi-Nejad, A.R., Ji, J.L., Howell, A., Rosand, B., Anticevic, A., Sotiropoulos, S.N., and Murray, J.D. (2024). On the stability of canonical correlation analysis and partial least squares with application to brain-behavior associations. Commun. Biol. *7*, 217.

79. Zhou, L., Saltoun, K., Marotta, J., Aggarwal, S., Kopal, J., Carrier, J., Storch, K.F., Dunbar, R., and Bzdok, D. (2025). Latent brain subtypes of chronotype reveal unique behavioral and health profiles across population cohorts. Nat. Commun. *16*, 11550.

80. McKinney, W. (2010). Data structures for statistical computing in Python. scipy *445*, 51–56.

81. Harris, C.R., Millman, K.J., Van Der Walt, S.J., Gommers, R., Virtanen, P., Cournapeau, D., Wieser, E., Taylor, J., Berg, S., Smith, N.J., et al. (2020). Array programming with NumPy. nature *585*, 357–362.

82. Waskom, M.L. (2021). Seaborn: statistical data visualization. J. Open Source Softw. *6*, 3021.

83. Hunter, J.D. (2007). Matplotlib: A 2D graphics environment. Comput. Sci. Eng. *9*, 90–95.

84. Pedregosa, F., Varoquaux, G., Gramfort, A., Michel, V., Thirion, B., Grisel, O., Blondel, M., Prettenhofer, P., Weiss, R., Dubourg, V., and Vanderplas, J. (2011). Scikit-learn: Machine learning in Python. J. Mach. Learn. Res. *12*, 2825–2830.

85. Virtanen, P., Gommers, R., Oliphant, T.E., Haberland, M., Reddy, T., Cournapeau, D., Burovski, E., Peterson, P., Weckesser, W., Bright, J., et al. (2020). SciPy 1.0: fundamental algorithms for scientific computing in Python. Nat. Methods *17*, 261–272.

86. Abraham, A., Pedregosa, F., Eickenberg, M., Gervais, P., Mueller, A., Kossaifi, J., Gramfort, A., Thirion, B., and Varoquaux, G. (2014). Machine learning for neuroimaging with scikit-learn. Front. Neuroinf. *8*, 14. https://doi.org/10.3389/fninf.2014.00014.

87. Tremblay-Mercier, J., Madjar, C., Das, S., Binette, A.P., Dyke, S.O., Étienne, P., Lafaille-Magnan, M.E., Remz, J., Bellec, P., Collins, D.L., et al. (2021). Open science datasets from PREVENT-AD, a longitudinal cohort of pre-symptomatic Alzheimer's disease. Neuroimage Clin. *31*, 102733.

88. Breitner, J.C., Wyse, B.W., Anthony, J.C., Welsh-Bohmer, K.A., Steffens, D.C., Norton, M.C., Tschanz, J.T., Plassman, B.L., Meyer, M.R., Skoog, I., et al. (1999). APOE-epsilon4 count predicts age when prevalence of AD increases, then declines: the Cache County Study. Neurology *53*, 321–331. https://doi.org/10.1212/wnl.53.2.321.

89. Huang, W., Qiu, C., von Strauss, E., Winblad, B., and Fratiglioni, L. (2004). APOE genotype, family history of dementia, and Alzheimer disease risk: a 6-year follow-up study. Arch. Neurol. *61*, 1930–1934. https://doi.org/10.1001/archneur.61.12.1930.

90. De Beaumont, L., Pelleieux, S., Lamarre-Théroux, L., Dea, D., and Poirier, J. (2016). Butyrylcholinesterase K and apolipoprotein E-ϵ4 reduce the age of onset of Alzheimer's disease, accelerate cognitive decline, and modulate donepezil response in mild cognitively impaired subjects. J. Alzheimers Dis. *54*, 913–922.

91. Gosselin, N., De Beaumont, L., Gagnon, K., Baril, A.A., Mongrain, V., Blais, H., Montplaisir, J., Gagnon, J.F., Pelleieux, S., Poirier, J., and Carrier, J. (2016). BDNF Val66Met polymorphism interacts with sleep consolidation to predict ability to create new declarative memories. J. Neurosci. *36*, 8390–8398.

92. Miron, J., Picard, C., Frappier, J., Dea, D., Théroux, L., and Poirier, J. (2018). TLR4 gene expression and pro-inflammatory cytokines in Alzheimer's disease and in response to hippocampal deafferentation in rodents. J. Alzheimers Dis. *63*, 1547–1556.

93. Miron, J., Picard, C., Labonté, A., Auld, D., Breitner, J., and Poirier, J. (2019). Association of PPP2R1A with Alzheimer's disease and specific cognitive domains. Neurobiol. Aging *81*, 234–243.

94. Miron, J., Picard, C., Nilsson, N., Frappier, J., Dea, D., Théroux, L., and Poirier, J. (2018). CDK5RAP2 gene and tau pathophysiology in late-onset sporadic Alzheimer's disease. Alzheimer's Dement. *14*, 787–796.

95. Welch, B.L. (1947). The generalization of 'STUDENT'S'problem when several different population varlances are involved. Biometrika *34*, 28–35.

STAR★METHODS

KEY RESOURCES TABLE

REAGENT or RESOURCE	SOURCE	IDENTIFIER
Deposited data		
PREVENT-AD Open Repository	Canadian Open Neuroscience Platform	ARK ID: https://n2t.net/ark:/70798/d78m93q8n7w4g20mhj
PREVENT-AD Registered Repository	Canadian Open Neuroscience Platform	ARK ID: https://n2t.net/ark:/70798/d7j9dvk4777m366kfb
Summary data and code	GitHub and Zenodo	https://github.com/chloesavignac/PREVENTAD https://doi.org/10.5281/zenodo.20355121
Software and algorithms		
Python 3.8.20, 3.12.2	Python Software Foundation	https://www.python.org
Pandas 1.5.3, 2.0.3	McKinney[80]	https://pypi.org/project/pandas/
Numpy 1.22.4, 1.26.4	Harris et al.[81]	https://pypi.org/project/numpy/
Seaborn 0.13.2	Waskom[82]	https://pypi.org/project/seaborn/
Matplotlib 3.9.2	Hunter[83]	https://pypi.org/project/matplotlib/
Scikit-learn 0.23.2, 1.4.1.post1	Pedregosa et al.[84]	https://pypi.org/project/scikit-learn/
Scipy 1.12.0	Virtanen et al.[85]	https://pypi.org/project/scipy/
Joblib 1.3.2, 1.4.2	The joblib developers. https://doi.org/10.5281/zenodo.14915601	https://pypi.org/project/joblib/
Nilearn 0.9.2, 0.10.4	Abraham et al.[86]; https://doi.org/10.5281/zenodo.21126970	https://pypi.org/project/nilearn/

EXPERIMENTAL MODEL AND STUDY PARTICIPANT DETAILS

Human participants

The PREVENT-AD cohort[87] is composed of older individuals with a known family history of Alzheimer's disease who were cognitively unimpaired at the time of enrollment from 2011 to 2017 (mean age 63, standard deviation [SD] 5 years). This susceptible population is estimated to have a 2- to 3-fold relative increase in the risk of AD-type dementia.[88,89] Sex and the affected AD parent's sex were self-reported by participants and are herein referred to as gender. Participants gave written, informed consent for the study, which was approved by the McGill Institutional Review Board and/or Douglas Mental Health University Institute Research Ethics Board. Further information on the consent procedure can be found elsewhere.[87] A study design chart, along with detailed information about data collection methods and data sharing plans, is openly available online.[87] Demographic information for the PREVENT-AD cohort (N = 384) stratified by *APOE* genotype is summarized in Table S20. All but four participants identified as Caucasian.

METHOD DETAILS

Non-imaging data preprocessing

The primary goal of PREVENT-AD is to test whether serial determination of multi-modal biomarkers of Alzheimer's disease may be measured and used in pre-symptomatic persons at high risk of subsequent AD dementia to trace the progression of the disease process and to measure effects of any potentially preventive treatment interventions. This work is intended to provide preliminary data regarding the probable efficacy and safety of potential new treatments for prevention of AD dementia. Participants of the PREVENT-AD initiative have undergone extensive annual health and cognitive assessments for up to five years. This resource creates a unique opportunity to monitor longitudinal trajectories of brain-imaging assessments, cerebral fluid biochemistry, neurosensory capacities, and medical charts in pre-symptomatic individuals at Alzheimer's risk. The risk markers included at the time of study design are thus inherently grounded in clinical practice, reflecting over 10 years of collective expertise in brain imaging, biochemistry, neuropsychology, genetics, and medicine. A complete list of the 257 risk indicators included in this study is available in the supplementary information (Table S21).

As part of the original PREVENT-AD study design, allelic variants of seven genes were pre-selected and genotyped by the original investigators based on prior evidence of association with AD available at the time.[27,90–94] The following allelic variants were genotyped and made publicly available to all future investigators: *APOE* (rs429358 and rs7412), *BDNF* (rs6265), *HMGCR* (rs3846662), *BCHE* (rs1803274), *TLR4* (rs4986790), *PPP2R1A* (rs10406151), and *CDK5RAP2* (rs10984186). All genetic variants preselected

and made available by the PREVENT-AD initiative were included in our models to extract intermediate phenotypes in an impartial, data-driven manner.

Our PREVENT-AD sample consisted of 384 participants (28.9% men, 71.1% women) with the following *APOE* genotype distribution: ϵ3/3 (50.8%), ϵ3/4 (32.0%), ϵ3/2 (10.9%), ϵ2/4 (4.2%), ϵ4/4 (2.1%). We first considered a total of 1,562 participant visits, from which we selected only those from participants with brain imaging and *APOE* genotyping information. Of those 910 visits, 109 came from participants with both maternal and paternal AD lineage and were excluded. An additional 62 visits that came from participants with only sibling history of AD were also excluded. We removed 57 visits from participants with ϵ4/4 (1 man/7 women) and ϵ2/4 (6 men/8 women) genotypes because of their limited sample sizes. We next balanced the percentage of men and women with ϵ3/2, ϵ3/3, and ϵ3/4 genotypes by dropping visits from women at random. We used the same procedure to balance the percentage of men and women with maternal and paternal AD lineage. A total of 250 visits from women were dropped in this procedure. In the final balanced sample, the distribution of *APOE* genotypes was the same in men and women and consisted of ϵ3/2 at 15%, ϵ3/4 at 35%, and ϵ3/3 at 50%. The distribution of maternal and paternal AD lineage in men and women was 34% paternal and 66% maternal. The final balanced sample consisted of 432 participant visits, 182 of which (42%) came from men.

Brain-imaging data preprocessing

Population-based cohorts are ideally suited to tease apart subregion-level variation in AD risk. Advances in automatic segmentation techniques for the human HC using *ex vivo* brain imaging have allowed for subject-specific parcellations that respect the diversity of distinct subregions identified postmortem.[51] Capitalizing on these ultra-high resolution segmentations, we previously assessed microstructural alterations of the human HC in a newly detailed way that scaled to ~40,000 UKB participants primarily of European genetic ancestry.[39] We described AD-related patterns of structural co-variation in DN subregions, which varied in lockstep with fine-grained HC subregions.[39] Working with the UKB enabled us to derive multivariate patterns of structural co-variation between 38 hippocampal subregions and 91 default network subregions—an analysis that is largely infeasible in most other neuroimaging cohorts due to sample size constraints.[78] While the UKB is uniquely powered to support such doubly multivariate decompositions, it was not designed to track AD progression. For this reason, we adopted a two-step dataset-bridging approach, building on previously established cross-cohort modeling strategies.[76,79] First, we derived HC–DN signatures in a large population-based cohort and then transferred these signatures to a specialized cohort of individuals at elevated risk for dementia, which offers rigorous longitudinal monitoring of AD progression in offspring of affected patients. By leveraging these complementary datasets, our approach allows us to assess the extent to which broadly distributed, population-derived neuroanatomical patterns generalize to clinically meaningful indicators of AD risk.

The PREVENT-AD resource provides brain imaging scanning (including T1-weighted images) for up to four years of follow-up from 386 participants. Separately for the brain-imaging scans from each participant visit, we first performed a full FreeSurfer reconstruction followed by subcortical volumetric sub-segmentation of the 38 hippocampal subfields, analogous to the UKB brain-imaging preprocessing pipeline. In the same way as in our previous publication, we next parsed the cortex volumes from the structural brain scans according to the Schaefer-Yeo parcellation (400 parcels, 7 networks) to obtain the analogous 91 parcels defined as belonging to the DN by the reference atlas (https://github.com/ThomasYeoLab/CBIG/tree/master/stable_projects/brain_parcellation/Schaefer2018_LocalGlobal/Parcellations/project_to_individual). Covariates (age, age,^{2} gender, gender*age, and gender*age^2) were regressed out from each brain-derived gray matter volume measure as part of the deconfounding procedure. Age was determined at the time of recruitment and gender was self-reported. The final brain-imaging sample consisted of 368 participants (261 women and 107 men) with a total of 912 individual visits.

We extracted the same collection of brain-image-derived phenotypes of gray matter morphology as our previous HC-DN co-variation study in the UKB.[39] We were thus able to compute the expression of the 25 UKB-derived modes of HC-DN co-variation based on gray matter measurements for the identical sets of 91 DN and 38 HC target subregions. For each PREVENT-AD visit, we obtained the subject-specific expression levels of the 25 HC and 25 DN patterns of structural co-variation (i.e., *canonical variates*) that capture the inter-individual variation in the 25 pairs of HC-DN co-variation signatures. These derived brain measures were fed into our downstream analyses.

QUANTIFICATION AND STATISTICAL ANALYSIS

Intermediate phenotypes of Alzheimer's disease risk

As the backbone of our analysis workflow, we sought to derive intermediate phenotypes (IPs) that partitioned the phenotypic expression of familial AD risk as a function of *APOE* genetic background. We capitalized on the rich PREVENT-AD indicators set to capture *APOE*-phenotypes associations across 257 risk indicators from 7 broad risk categories: cardiovascular health, cognition, clinical comorbidities, demographics, disease progression, genetics, and neurosensory assessments. We designed PLS-regression (PLS-R) models in which the *APOE* genotypes (e.g., ϵ3/2, ϵ3/3, ϵ3/4) were estimated based on these 257 risk indicators. PLS-R was a natural choice of method as it is especially suited to disentangle the variance of a high-dimensional set as a function of a targeted outcome. Because PLS-R estimates latent components by maximizing shared covariance across variable blocks, correlated predictors are consolidated into composite constructs (i.e., *intermediate phenotypes*) rather than treated as competing independent regressors.

As a result, the approach is inherently robust to problems emerging from collinearity and enables shared environmental factors to be modeled directly within the multivariate structure, rather than statistically controlled or residualized out.

The explanatory input variable set X was constructed from the PREVENT-AD risk indicators (number of subject visits × 257 phenotypes). A parallel outcome variable set Y was constructed from the one-hot-encoded *APOE* genotypes (number of subject visits × 3 genotypes (e.g., ϵ3/2, ϵ3/3, ϵ3/4)):

$$X \in \mathbb{R}^{n \times m} \text{ and}$$

$$Y \in \mathbb{R}^{n \times p},$$

where m denotes the number of PREVENT-AD phenotypes, and p the number of *APOE* genotypes. PLS-R finds latent variables that model X and simultaneously predict Y. The two sets X and Y are decomposed as the dot product of two matrices that represent the model scores (T,U), and loadings (P,Q), respectively. The decomposition of the original variable sets is obtained as follows:

$$X = TP^T + E,$$

$$Y = UQ^T + F,$$

$$T = XW^*, \text{and}$$

where T and U are matrices of size $n \times l$, P is a matrix of size $m \times l$, Q is a matrix of size $p \times l$, and E and F are matrices of normally distributed error terms for X and Y, respectively. The number of loadings is denoted by l and determined by the rank of X. Following the principle of linear regression, Y can be estimated as a function of X through the following equation:

$$Y = TQ^T + G,$$

where G is a matrix of normally distributed residuals. This equation can be re-expressed as the multiple regression model:

$$Y = XW^*Q^T + F \text{ and}$$

$$B = W^*Q^T,$$

where B is a matrix of regression weights, equivalent to the coefficients of a multiple regression model. PLS-R thus find a series of L orthogonal latent variables, i.e., t_l, that have maximal covariance with Y but are uncorrelated to each other. These latent variables are ordered according to the amount of variance of Y that they explain. Formally, the optimization can be described as follows:

$$t_l = Xw_l, \text{such that } cov(t_l, Y) = max.$$

We apply a one-sample bootstrap hypothesis test to determine the number of robust, statistically meaningful PLS-R components. For 1,000 iterations, we randomly sampled participant visits with replacement to create alternative datasets we could have gotten. At each iteration, we recomputed the PLS-R solution. We averaged the PLS-R loadings of each of the 257 PREVENT-AD indicators at each of the 1,000 iterations and compared them with the actual loadings of the original unshuffled PLS-R model. The degree of consistency between the original PLS-R loadings and the average bootstrapped loadings was assessed using Pearson's correlation. (see Figure S4). We found that the robustness of the PLS-R solution substantially dropped after the third PLS-R component (Pearson's $\rho < 0.50$). In contrast, the first 3 PLS-R components showed robust convergence: component 1 (Pearson's $\rho = 0.988$, p value = 8.6×10^{-208}), component 2 (Pearson's $\rho = 0.793$, p value = 7.4×10^{-57}), and component 3 (Pearson's $\rho = 0.778$, p value = 1.7×10^{-53}). For that reason, we only considered the first three PLS-R components for all downstream analyses.

Assessment of lineage and gender biases

We next systematically examined how gender and parental lineage relate to the IPs. Each intermediate phenotype captures a distinct portion of the phenome-wide variation in AD risk associated with the *APOE* gene. We aimed to systematically examine the 257 risk factors to identify those that show the greatest variation in their association with *APOE* genotypes, as a function of gender and parental history of AD. To this end, we conducted parallel analyses in which analogous intermediate phenotypes were derived separately for men and women, and for individuals with maternal vs. paternal AD history. This allowed us to assess which components of phenome-wide AD risk variation can be attributed to gender and family lineage. Specifically, we compared the weights of individual risk factors across subgroups to identify how their relative contributions to each of the three intermediate phenotypes differed by gender and lineage.

We first stratified the dataset by gender and by parental AD lineage. Specifically, we separated men ($n = 182$) and women ($n = 250$) subject visits and built two gender-specific PLS-R models, using the standardized 257 PREVENT-AD risk indicators to estimate *APOE* genotypes (ϵ3/2, ϵ3/3, ϵ3/4). In parallel, we built analogous models for individuals with maternal ($n = 284$) and paternal ($n = 148$) AD lineage. As previously described (see "Non-imaging data preprocessing"), the distributions of *APOE* genotypes and parental AD lineage were balanced across genders.

Please cite this article in press as: Savignac et al., Parent-of-origin effects in Alzheimer's liability dissociate neurocognitive and cardiovascular traits in at-risk individuals, Cell Reports Medicine (2026), https://doi.org/10.1016/j.xcrm.2026.102943

Our goal was to quantitatively compare the contribution (i.e., weights) of each risk factor across these stratified models, to determine which indicators showed the most gender- or lineage-specific variation in their association with *APOE* genotype, which, by itself, accounts for over 90% of the predictive accuracy of the genetic risk score for AD.[17] To ensure alignment of the PLS-R components being compared, we computed Pearson's correlation coefficients between the y-loadings—that is, the weights of the three most prevalent *APOE* genotypes—from the first five PLS components of each subgroup (e.g., men vs. women, maternal vs. paternal lineage) and those from the original PLS run on the entire balanced sample. Components were hierarchically matched based on these correlations, then reordered and sign-corrected to ensure that each matched component represented a biologically comparable genotype-associated axis of variation. Once aligned, we subtracted the x-loadings (i.e., the weights of the 257 risk indicators) of the first three matched PLS components between subgroups. This yielded phenotype-level estimates of gender-specific and lineage-specific differences in AD risk. Through this procedure, we identified which PREVENT-AD risk indicators contributed most to variation in AD susceptibility as a function of gender and parental lineage.

To robustly assess gender and lineage differences in *APOE*-related risk profiles, we performed a nonparametric bootstrap procedure with as many as 1,000 iterations. In each iteration, we randomly resampled participant visits with replacement, generating alternative datasets drawn from the original distribution. For each resampled dataset, we recalculated the PLS-R models separately for men and women, and for individuals with maternal vs. paternal history of AD. Components were then reordered and sign-corrected within each iteration to match the corresponding components from the original PLS (cf. above).

From each bootstrap sample, we extracted the x-loadings—that is, the contribution of each of the 257 PREVENT-AD risk factors—for each aligned PLS component in each subgroup. These values were aggregated across iterations to produce density plots that illustrate the distribution of gender- and lineage-specific loadings across all bootstrap iterations (see Figures S8 and S9; Tables S14–S19). To complement this machine learning–based approach with classical statistical inference, we computed standardized effect sizes and statistical tests for each group comparison (i.e., men vs. women; maternal vs. paternal lineage). Specifically, we calculated Cohen's d and performed Welch's unequal variances *t* test using the scipy.stats.ttest_rel() function from the SciPy library. This test assesses whether two related or repeated samples differ significantly in their mean values.[95]

Together, the bootstrap resampling and classical statistical analyses aim to confirm that the observed gender and lineage differences in intermediate phenotype composition are not due to random variation or outliers, but instead reflect robust, reproducible associations with *APOE* genotype.

Longitudinal risk analysis

We examined how the gender-specific and lineage-specific variation in AD risk captured by the three IPs changed over time. We capitalized on the serial assessments of the PREVENT-AD cohort to track category-wise progression in AD risk over a 4-year follow-up period. That way, we were able to identify which of the 7 broad categories of AD risk factors (cf. above) track most of the gender-specific and lineage-specific fluctuation in AD risk for a given intermediate phenotype.

The balanced sample comprised 432 subject visits from 233 different PREVENT-AD participants, with 126 participants (55% women, 65% maternal AD lineage) having at least one follow-up visit over a 4-year period. For each participant with follow-up data, we used their first and last visits as the two time points for analysis. We ran gender-specific and lineage-specific PLS-R models separately for each time point, enabling us to extract the intermediate phenotypes at both the initial and last follow-up visits, which provided the basis for our longitudinal analysis.

To compare how these intermediate phenotypes evolved over time, we matched the PLS-R components across the four subgroups (men vs. women and maternal vs. paternal AD lineage), and two time points. To do so, we computed Pearson's correlation coefficients between the y-loadings (i.e., the weights of the three most prevalent *APOE* genotypes) for the first five PLS-R components across the subgroups we aimed to compare and the original PLS, run on the entire balanced sample. This step ensured that the PLS-R components were biologically comparable by verifying their association with corresponding *APOE* genotypes. Once we obtained the Pearson's correlation matrices, we reordered the components in the comparison subgroups based on the strength of their correlation with the corresponding components in the original PLS.

After ordering and aligning the components using this procedure, we subtracted the x-loadings for men and women, as well as for maternal and paternal lineages, to derive category-specific estimates of generational differences in AD risk. This approach allowed us to pinpoint which PREVENT-AD risk indicators exhibited the most significant gender-specific and lineage-specific variation within a given IP.

Finally, we averaged the differences in x-loadings by gender and AD lineage for each of the seven categories of risk indicators—cardiovascular health, cognition, clinical comorbidities, demographics, disease progression, genetics, and neurosensory assessments—at both time points. This approach provided us with category-specific estimates of gender- and lineage-specific differences in AD progression for each of the three intermediate phenotypes.

Region-wise brain imaging analyses

Next, we assessed whether maternal vs. paternal AD lineage is linked to specific structural variation in HC and DN subregions defined above (see Brain-imaging data preprocessing). More specifically, we wanted to quantify how much a given subregion contributes to the classification of maternal vs. paternal AD risk in the context of the whole set of 38 HC subregions or 91 DN subregions. This

Please cite this article in press as: Savignac et al., Parent-of-origin effects in Alzheimer's liability dissociate neurocognitive and cardiovascular traits in at-risk individuals, Cell Reports Medicine (2026), https://doi.org/10.1016/j.xcrm.2026.102943

diagnostic test enabled us to pin down which (if any) microstructurally defined subregions within two cortical systems broadly affected in AD were related to either maternal or paternal AD lineage.

We built classification models (logistic regression) to estimate the type of AD lineage (maternal = 1, paternal = 0) as a function of gray matter volumes in the 38 HC subregions of the FreeSurfer subcortical atlas (see Brain-imaging data preprocessing). Two separate lineage-classification models were built, one for men and one for women. Each classifier considered 38 input variables corresponding to the gray matter volumes in the HC subregions. We employed a resampling procedure to account for differences in the numbers of men vs. women, and individuals with maternal vs. paternal AD lineage, that could affect classification toward to most prevalent classes. Across 1,000 iterations, we randomly drawn visits from 100 men and 100 women, half of which had a history of AD on their mother's side, while the other half had an history of AD on their father's side, from 912 visits with MRI measurements (see Brain-imaging data preprocessing). We obtained 1,000 different subsamples where men and women with maternal and paternal AD lineage were equally represented. At each iteration, we randomly shuffled the true outcome of the classification model (maternal = 1, paternal = 0) 1,000 times and recomputed the classification weights for each resampled subject dataset. In so doing, we could empirically derive null distributions for the 38 coefficients of the 1,000 subsamples on which we performed two-tail tests for statistical relevance. The analogous classification and resampling analyses were conducted on the set of 91 default network subregions.

Lineage and gender biases in brain signatures

We next tested whether our UKB-derived signatures of HC-DN co-variation relate to the PREVENT-AD-derived intermediate phenotypes in classifying the type of AD lineage. Capitalizing on these two independently collected datasets allowed us to identify clinically relevant aspects of AD risk robustly tracked by the HC-DN co-variation signatures. We aimed to build upon the characterization of our population-derived limbic-cortical regimes by linking them with widely established indicators of dementia progression in presymptomatic individuals. We examined whether we could differentiate the type of AD lineage based on a set of explanatory input variables including i) the three PREVENT-AD-derived intermediate phenotypes, ii) individual variation in expression of 25 HC-DN co-variation patterns (i.e., canonical variates), and iii) the interaction between the three intermediate phenotypes and the 25 co-variation pattern expression strengths. For each gender, we built separate classification models for each of the 25 HC and 25 DN canonical variates, yielding a total of 50 estimated models per gender. In each model, the type of AD lineage (encoded as 0 for paternal and 1 for maternal) was regressed on one HC or DN canonical variate, the three PREVENT-AD-derived intermediate phenotypes, and three interaction terms capturing possible non-linear association between each of the three intermediate phenotypes and the given HC or DN pattern, for a total of 7 regression parameters. We thus obtained a total of 100 logistic model fits that sought to explain variance in the family history of ADRD as a function of these 7 parameters.

As a complementary analysis integrating across the obtained classification models, we performed a permutation analysis to assess the robustness of each of the 7 classification coefficients. In 1,000 iterations, we randomly shuffled the type of AD lineage (maternal = 1, paternal = 0) across the 432 participant visits of the balanced sample. We recomputed the otherwise identical classification models based on the data with randomized outcomes. We recorded the classification coefficients from each of the 1,000 iterations and used them to build empirical null distributions which provided the basis to perform two-tail statistical tests at a 95% confidence level.

Back projection of brain-phenotype interaction

Lastly, we sought to quantify how matri-vs. patrilineal AD risk captured by the PREVENT-AD-derived intermediate phenotypes were expressed in AD-vulnerable brain structures. We used the interaction terms from the 100 classification models (50 per gender, cf. above) to derived estimates of brain-phenotype associations pooled across AD lineage. The interaction terms encapsulate how much a given HC or DN co-variation patterns is linked to a given intermediate phenotype of AD susceptibility in the context of maternal vs. paternal AD risk. We could then quantify how much of the brain-phenotypic variation captured by a given intermediate phenotype is reflected in anatomically defined HC and DN subregions.

We multiplied the interaction terms between a given IP and a given HC or DN pattern by the subject-specific expressions of that same pattern. For each subject visit, we obtained 50 brain-phenotype association terms corresponding to the original pairs of 25 HC-DN brain signatures pooled across the variance in AD lineage explained by a given IP. We projected back the 50 brain-phenotype association terms onto brain space by multiplying them with the respective 38 HC and 91 DN loadings of the original UKB-derived CCA model.[39] In doing so, we were able to assess the individual contribution of each of the original 38 HC and 91 DN subregions to brain-phenotype associations captured by the three IPs.

Cell Reports Medicine, Volume *7*

Supplemental information

Parent-of-origin effects in Alzheimer's liability dissociate neurocognitive and cardiovascular traits in at-risk individuals

Chloé Savignac, Frédéric St-Onge, Sylvia Villeneuve, AmanPreet Badhwar, Sarah A. Gagliano Taliun, Sali Farhan, Maiya Geddes, Yasser Iturria Medina, Judes Poirier, R. Nathan Spreng, Danilo Bzdok, and PREVENT-AD Research Group

This PDF file includes:

Supplementary Figures S1-S13.
Supplementary Table S20.

Other supporting materials for this manuscript include the following:

Supplementary Tables S14-S19 & S21.

Supplementary Figures

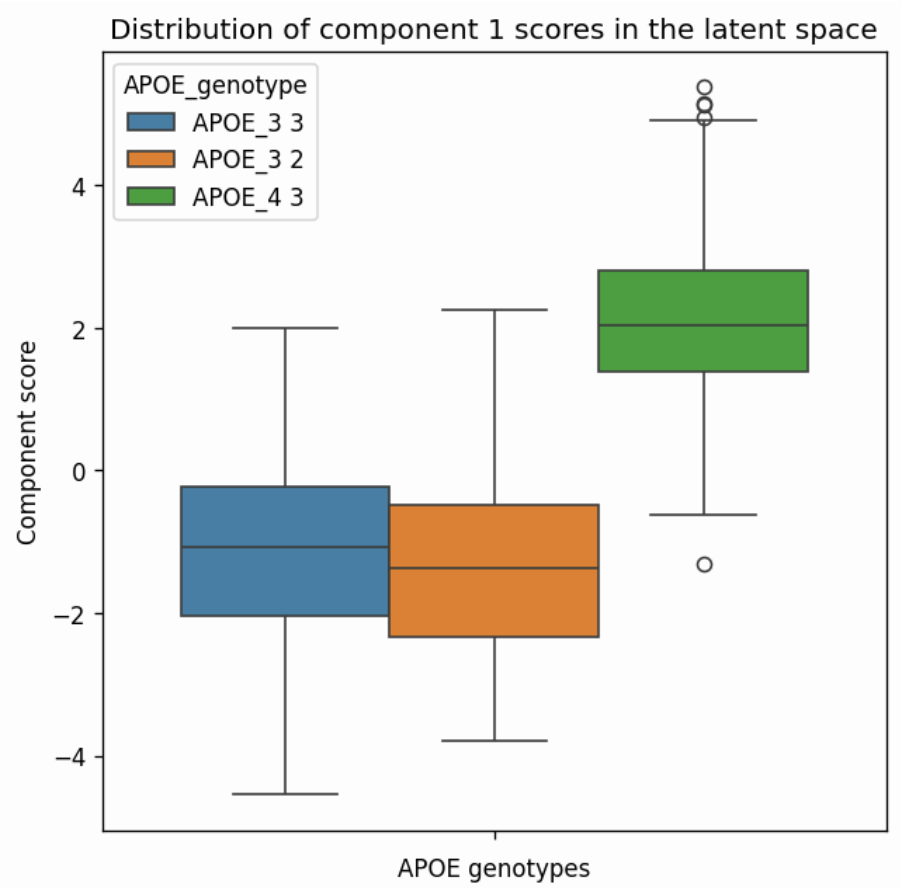

S1. Box plot for the first intermediate phenotype, related to Figure 2. We show the distribution of the scores from the first PLS-R component, i.e., the first intermediate phenotype of AD liability, for the three *APOE* genotype groups analyzed. We found that the interquartile range is of similar size across all three *APOE* genotype groups. This finding suggests that the variance explained in high dimensionality by the first intermediate phenotype is the same across all three *APOE* groups. We also show that the scores for *APOE* ε4/3 are higher than for the other two genotypes. This is consistent with the *APOE* loadings for the first intermediate phenotype (see Figure 2) that shows a stronger weight for *APOE* ε4/3 (0.38) than for ε3/3 (-0.27) and ε3/2 (-0.13).

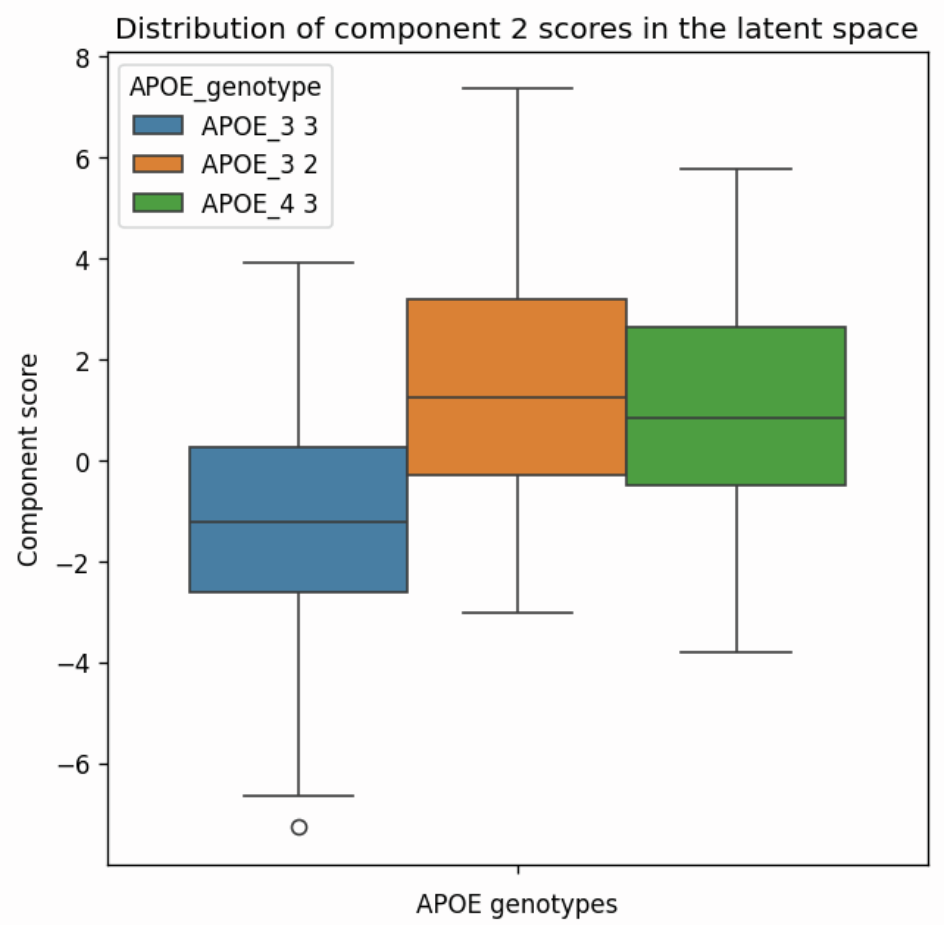

S2. Box plot for the second intermediate phenotype, related to Figure 3. We show the distribution of the scores from the second PLS-R component, i.e., the second intermediate phenotype of AD liability, for the three *APOE* genotype groups analyzed. We found that the interquartile range is of similar size across all three *APOE* genotype groups. This finding suggests that the variance explained in high dimensionality by the second intermediate phenotype is the same across all three *APOE* groups. We also show that the median score for the *APOE* ε3/3 group is of opposite sign than for the other two genotype groups. This is consistent with the *APOE* loadings for the second intermediate phenotype (see Figure 3) that shows a negative weight for *APOE* ε3/3 (-0.19) and positive weights for ε3/2 (0.10) and ε3/4 (0.13).

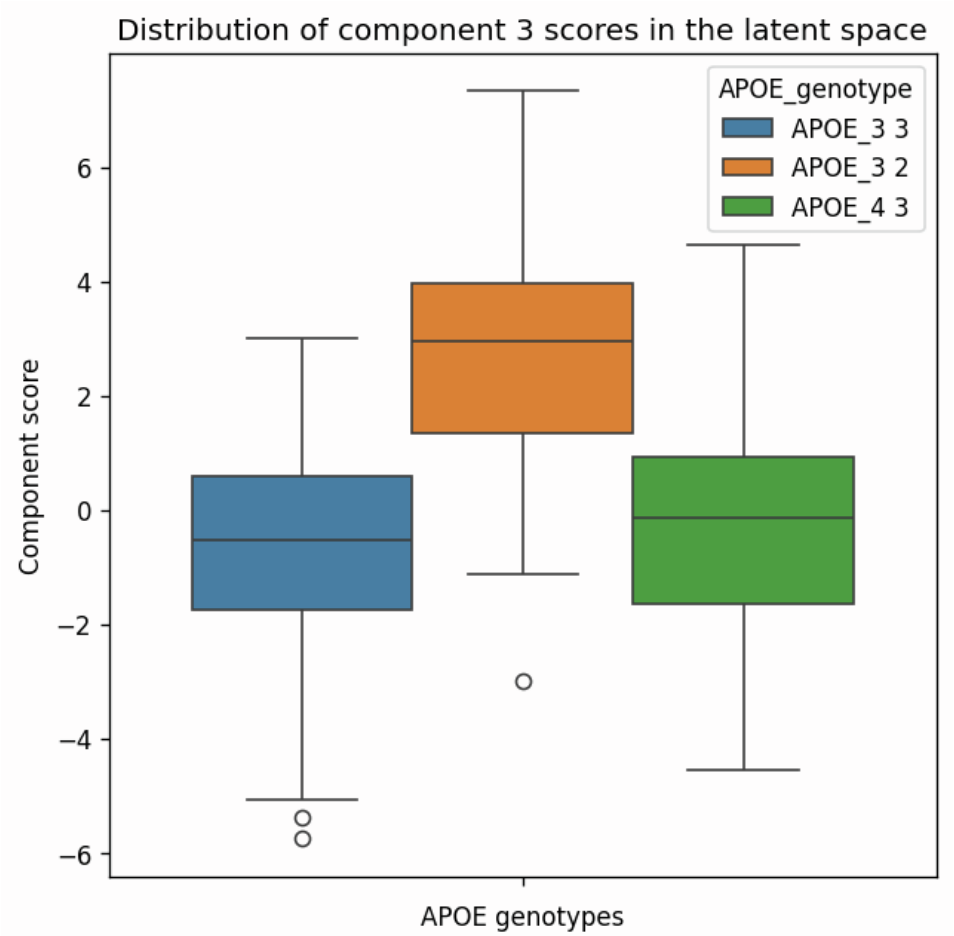

S3. Box plot for the third intermediate phenotype, related to Figure 4. We show the distribution of the scores from the third PLS-R component, i.e., the third intermediate phenotype of AD liability, for the three *APOE* genotype groups analyzed. We found that the interquartile range is of similar size across all three *APOE* genotype groups. This finding suggests that the variance explained in high dimensionality by the third intermediate phenotype is the same across all three *APOE* groups. We also show that the scores for *APOE* ε2/3 are higher than for the other two genotypes. This is consistent with the *APOE* loadings for the third intermediate phenotype (see Figure 4) that shows a stronger weight for *APOE* ε2/3 (0.26) than for ε3/4 (-0.04) and ε3/3 (-0.14).

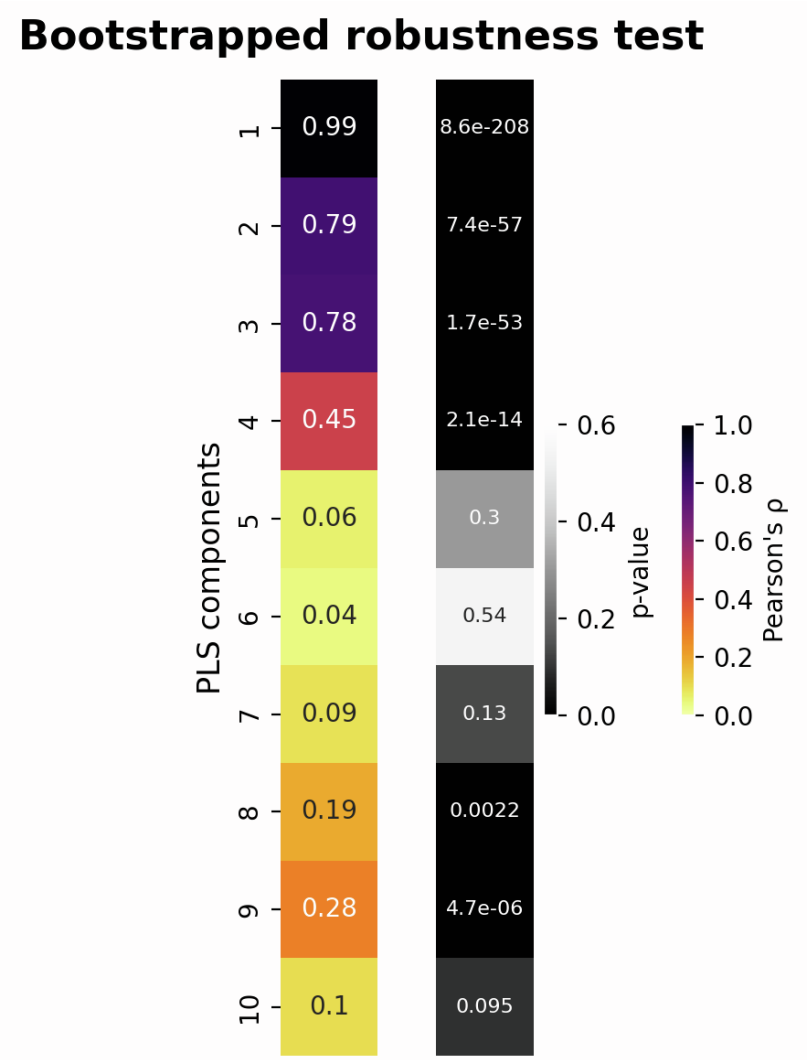

S4. Results of the bootstrapped procedure, related to Figures 2-4. To assess the robustness of the PLS-R solution, we performed 1,000 bootstrap iterations, each involving random sampling with replacement of participant visits and recomputation of the PLS-R solution. For each iteration, we averaged the PLS-R loadings of the 256 PREVENT-AD indicators and compared these bootstrapped averages with the original PLS-R loadings. The degree of consistency was measured using Pearson's correlation coefficient. Results show that the robustness of the PLS-R solution significantly declined beyond the third component (Pearson's ρ<0.50). In contrast, the first 3 PLS-R components showed robust convergence: component 1 (Pearson's ρ=0.988, p-value=8.6×10^{-208}), component 2 (Pearson's ρ=0.793, p-value=7.4×10^{-57}), and component 3 (Pearson's ρ=0.778, p-value=1.7×10^{-53}).

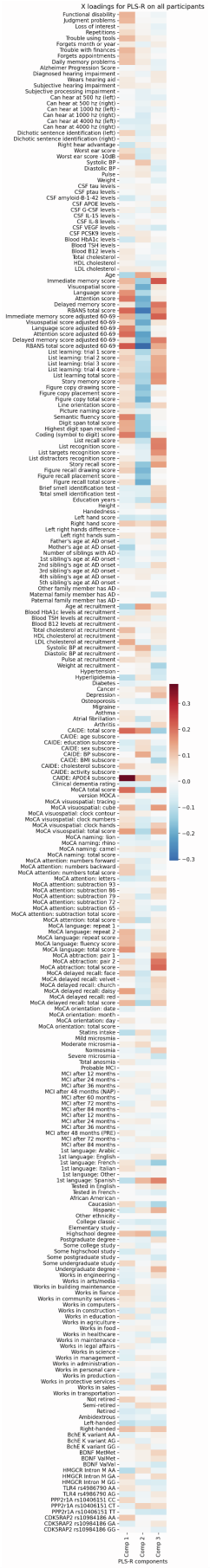

S5. PLS-R loadings for the 257 PREVENT-AD phenotypes, related to Figures 2-4. Full list of PLS-R loadings for the 257 PREVENT-AD phenotypes on the first three leading components.

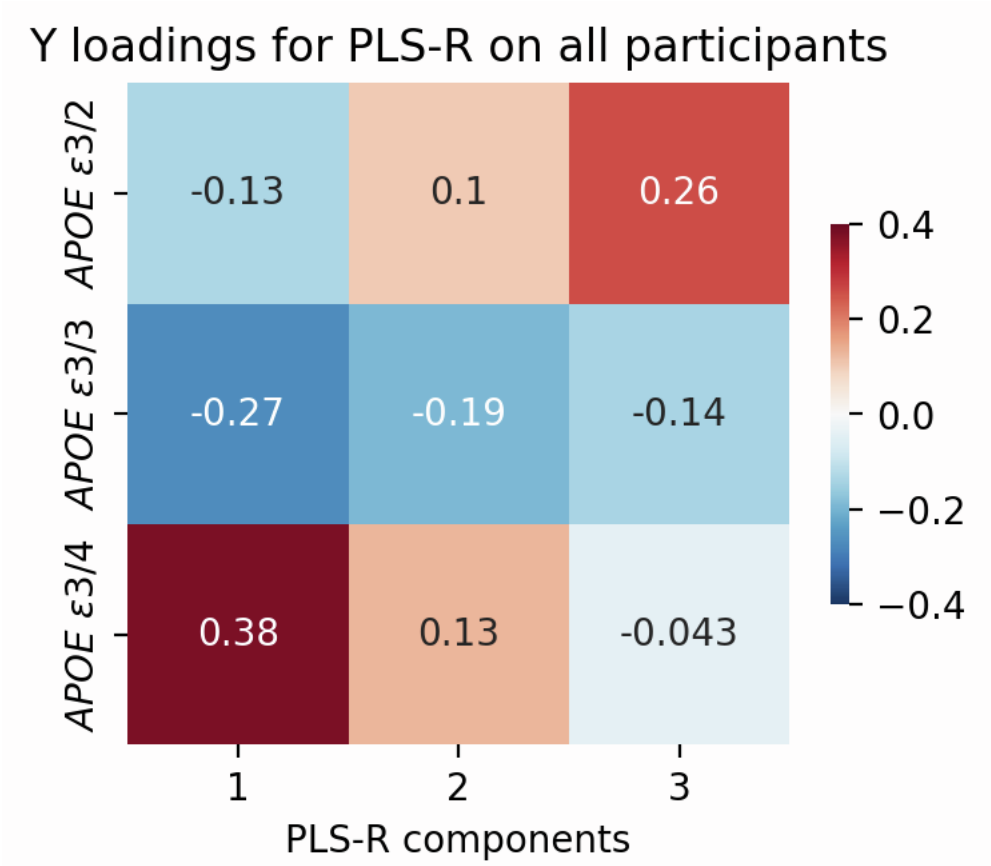

S6. PLS-R loadings for the *APOE* genotypes, related to Figures 2-4. Respective value of the loadings for each one-hot-encoded *APOE* genotypes on the first three leading PLS-R components.

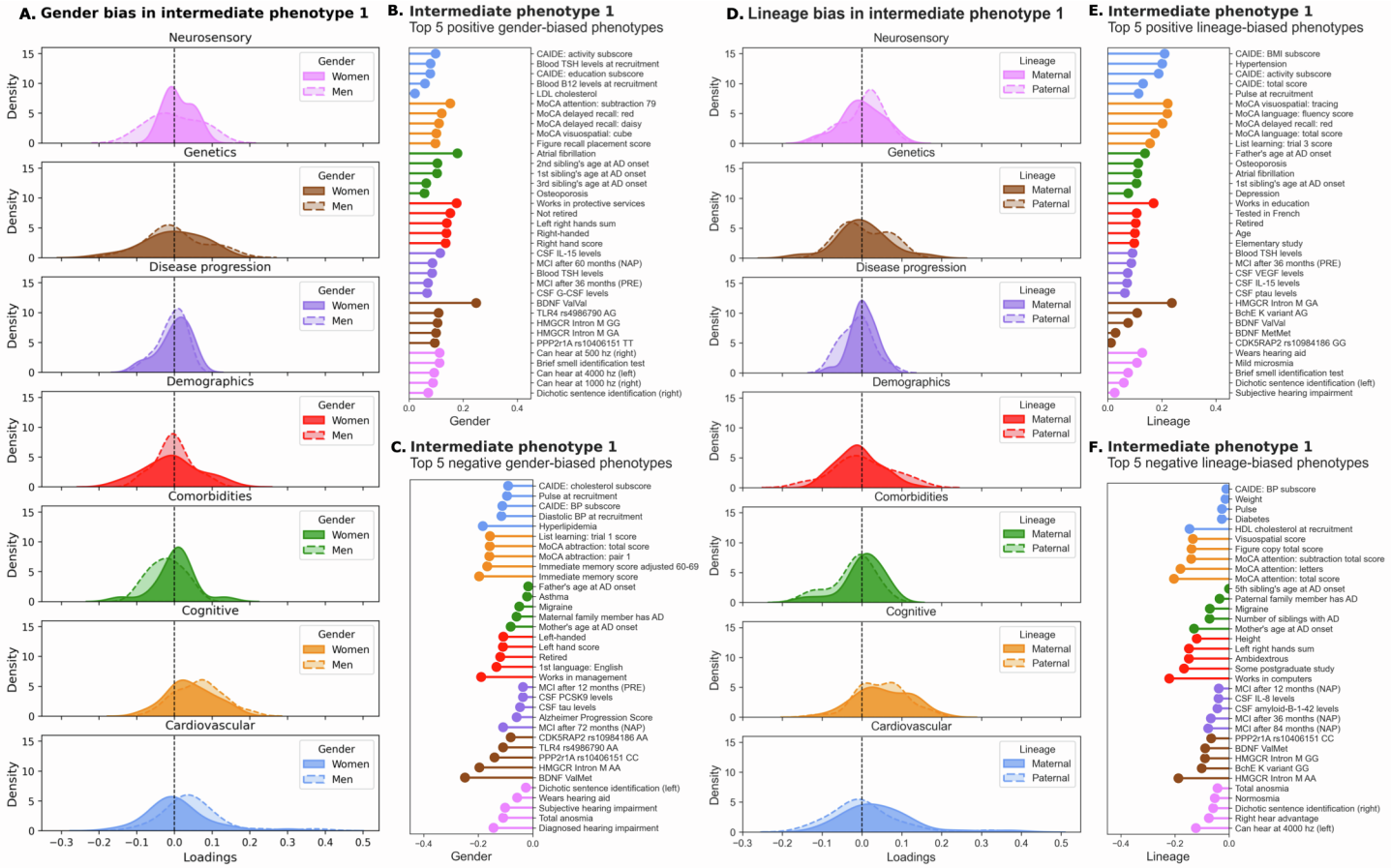

S7. Breakdown of lineage- and gender-specific biases for intermediate phenotype 1, related to Figure 2. The distribution of PLS loadings across the six categories of risk indicators is shown for the first intermediate phenotype in (A) men and women and (D) individuals with maternal and paternal AD lineage. Additional per-category breakdowns of loading differences are shown by gender in (B & C) and by AD lineage in (E & F). *BDNF* Val/Val and Val/Met genotypes show the strongest gender-biased genetic risk signals, varying in opposite directions along the AD liability spectrum captured by intermediate phenotype 1 (panels B & C). SNP rs3846662, located in intron M of the *HMGCR* gene, exhibits the most pronounced lineage bias among genetic risk indicators (panels E & F). Maternal and paternal ages at onset, used as proxies for parent-of-origin effects in AD and other conditions, emerge as the leading lineage-diverging variables within the comorbidity domain, again showing opposing trends across the AD liability spectrum (panels E & F). Overall, the first intermediate phenotype of AD susceptibility captures cross-generational differences in genetic risk, particularly in pathways related to memory and lipid metabolism, with the opposing maternal and paternal age-at-onset patterns further supporting parent-of-origin effects.

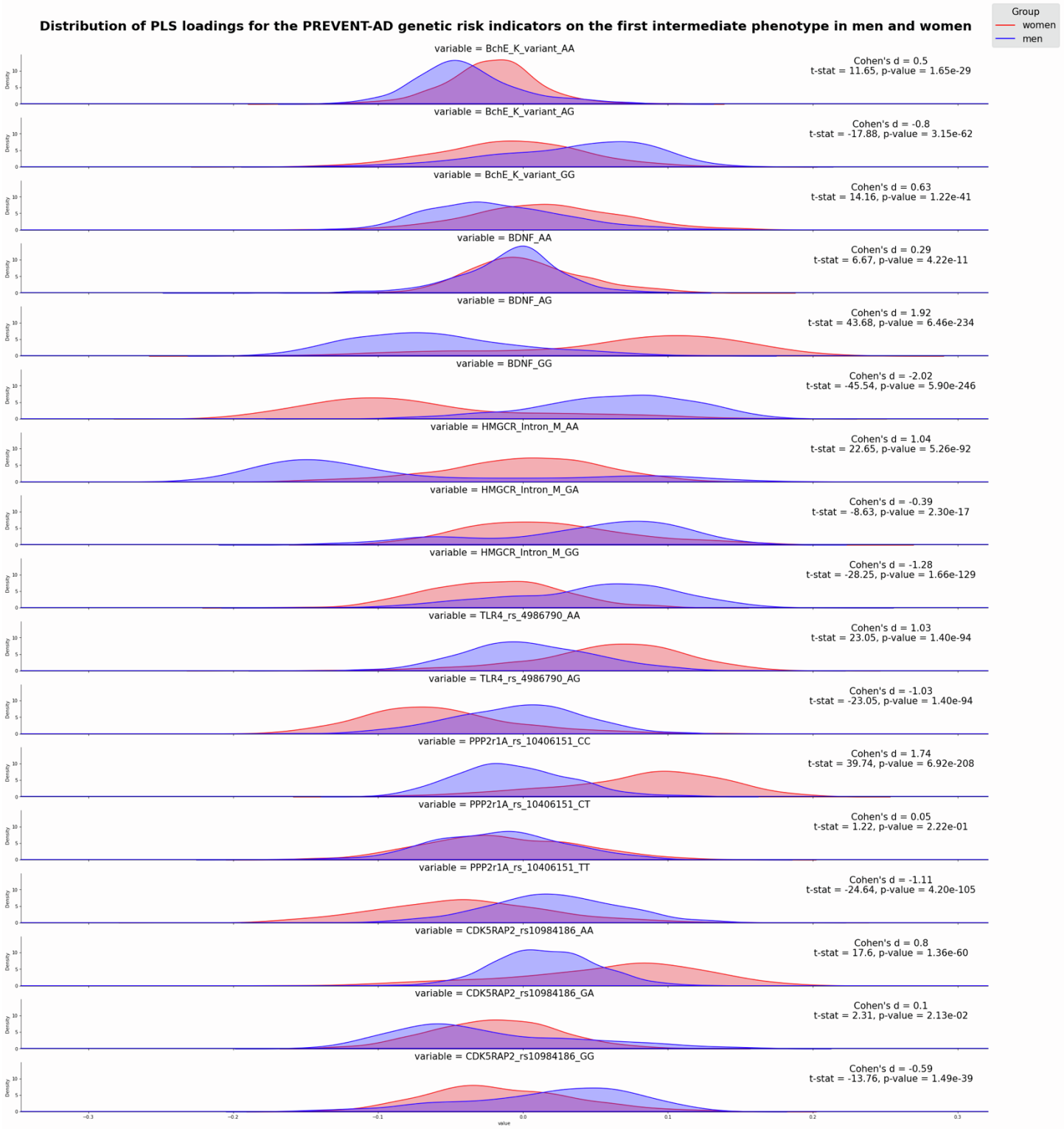

S8. *BDNF* ValVal and ValMet polymorphisms show robust differences between men and women, related to Figure 2. Bootstrapped density plots of the PLS-R loadings for the PREVENT-AD genetic risk indicators on the first intermediate phenotype in men and women revealed robust gender bias in *BDNF* variants ValVal (Cohen's d=-2.02; t-stat=-45.54, p-value=5.90×10^{-246}) and ValMet (Cohen's d=1.92; t-stat=43.68, p-value=6.46×10^{-234}).

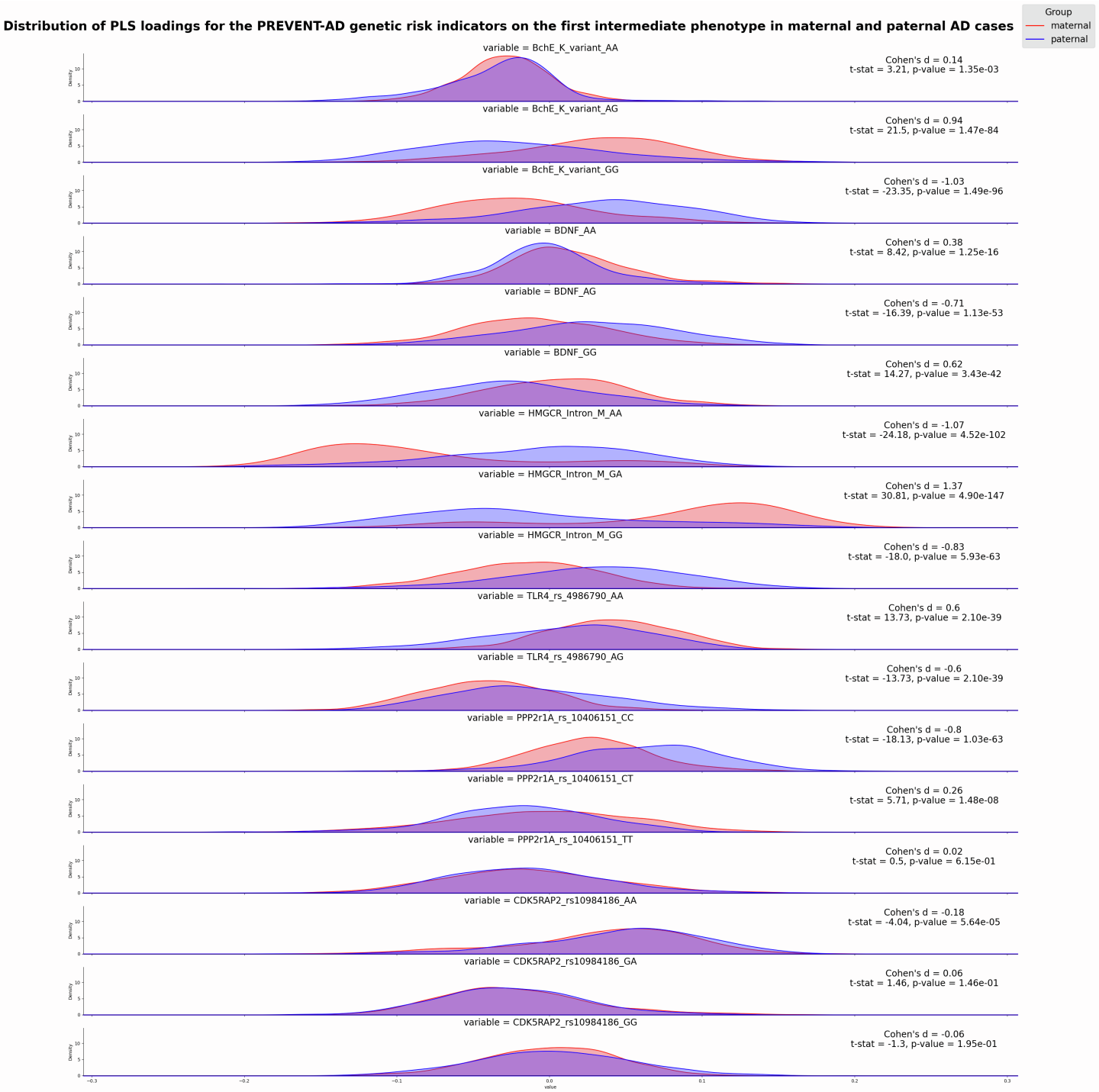

S9. Polymorphism in intron M of the *HMGCR* gene show robust AD lineage bias, related to Figure 2. Bootstrapped density plots of the PLS-R loadings for the PREVENT-AD genetic risk indicators on the first intermediate phenotype in individuals with maternal and paternal AD risk revealed a robust lineage difference on *HMGCR* G/A (Cohen's d=1.37; t-stat=30.81, p-value=4.90×10^{-147}) and A/A (Cohen's d=-1.07; t-stat=-24.18, p-value=4.52×10^{-102}).

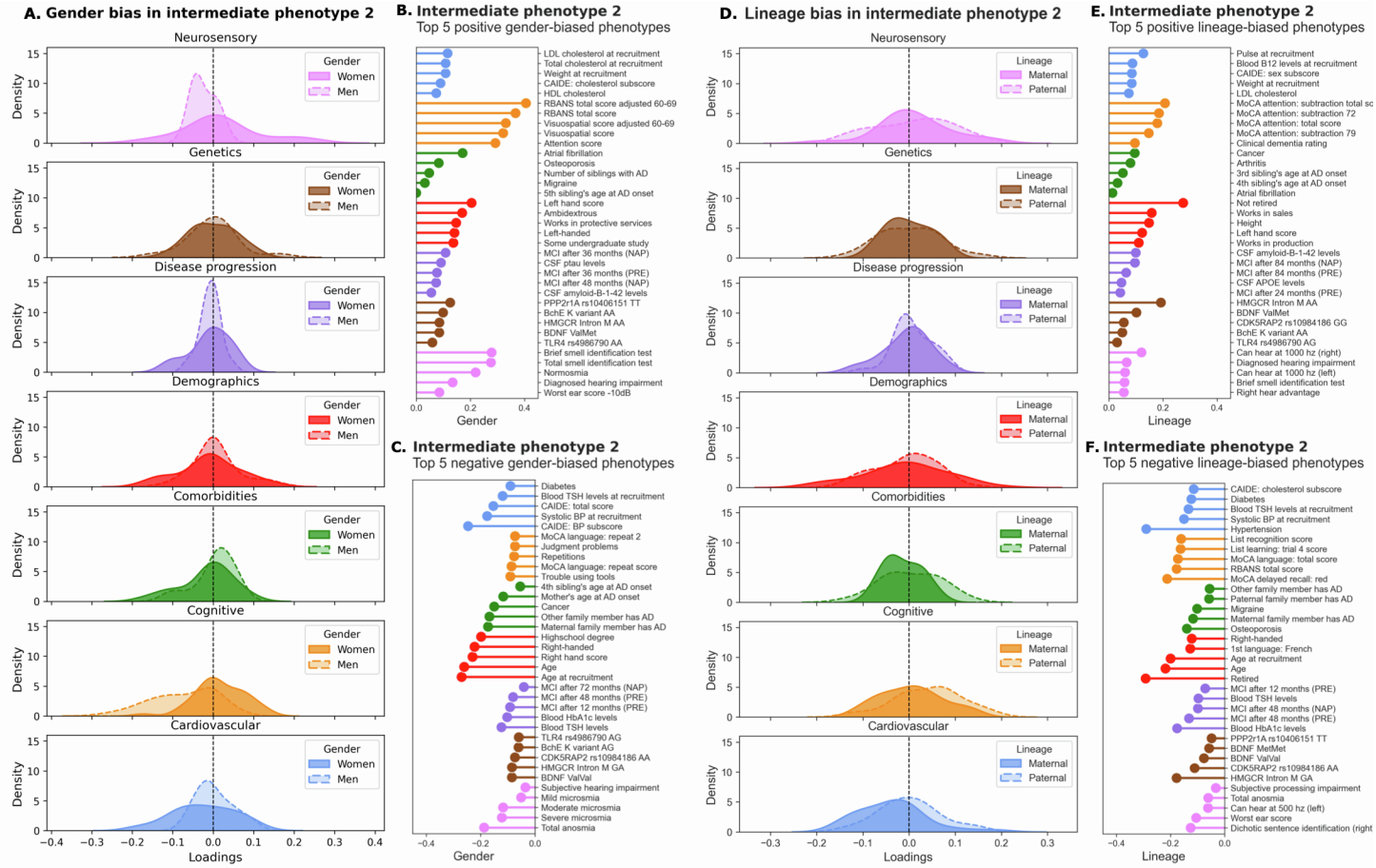

S10. Breakdown of lineage- and gender-specific biases for intermediate phenotype 2, related to Figure 3. The distribution of PLS loadings across the six categories of risk indicators is shown for the second intermediate phenotype in (A) men and women and (D) individuals with maternal and paternal AD lineage. Additional per-category breakdowns of loading differences are shown by gender in (B & C) and by AD lineage in (E & F). This intermediate phenotype distinguished *APOE* ε3 homozygotes from ε2 and ε4 carriers (Figure 3). Although ε3 homozygotes are typically used as a reference group in AD research—often assumed to reflect normative aging—we observe substantial gender- and lineage-specific biases in cognitive risk within this group. Among the most robust findings, global cognition, as assessed by the Repeatable Battery for the Assessment of Neuropsychological Status (RBANS), consistently ranked among the top contributors in both comparisons, showing pronounced gender (panels B & C) and lineage effects (panels E & F). Visuospatial processing was particularly influenced by gender (panel B), whereas working memory—as assessed through the Montreal Cognitive Assessment (MoCA) attention tasks—exhibited pronounced lineage effects (panel E). Age-related markers, including chronological age, retirement status, and hypertension, similarly exhibited notable gender (panels B & C) and lineage effects (panels E & F). Overall, these results indicate that even the baseline genetic risk group displays marked gender- and lineage-dependent variation in AD-related vulnerability.

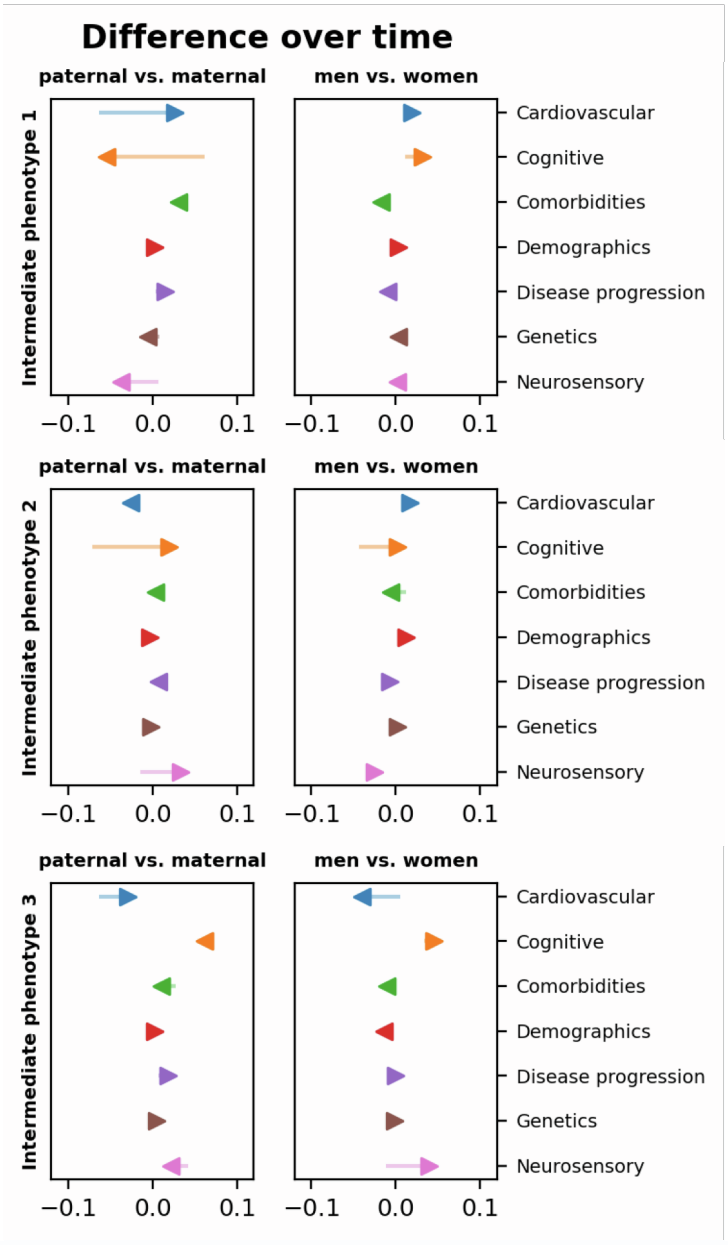

S11. Average category-wise difference in gene module loadings over time, related to Figures 2-4. We leveraged the longitudinal design of the PREVENT-AD cohort to track changes in AD risk indicators over a 4-year period. We used data from their first and last visits of each participant with at least one follow-up visit (N=126; 55% women; 65% maternal AD lineage). We computed separate gender-specific and lineage-specific PLS-R models at each time point to assess the expression of the three intermediate phenotypes over time. We show the average differences in x-loadings between men vs. women and maternal vs. paternal lineage within each of the seven risk categories. In the first intermediate phenotype, cardiovascular and cognitive risk indicators showed inverse variation over time with regards to AD lineage. This suggests that individuals with maternal and paternal AD lineage differ, in opposite directions, with regards to their average trajectory in cognitive and cardiovascular health. In the second intermediate phenotype, the lineage biases decreased over time, suggesting that the effects of maternal and paternal AD lineage on cognition ultimately converge with regards to the *APOE* ε3 allele. The third intermediate phenotype showed increasing gender-related but decreasing lineage-related biases in cardiovascular risk indicators over the follow-up period. Gender biases in neurosensory risk increased over time, but in the opposite direction to those observed for cardiovascular risk. Longitudinal monitoring of intermediate phenotypes offers valuable insight into how early-life genetic and familial factors interact with aging processes to influence susceptibility trajectories. These findings imply that AD risk is not static but shifts dynamically with age, and that gender and parental lineage shape these changes differently across multiple risk domains.

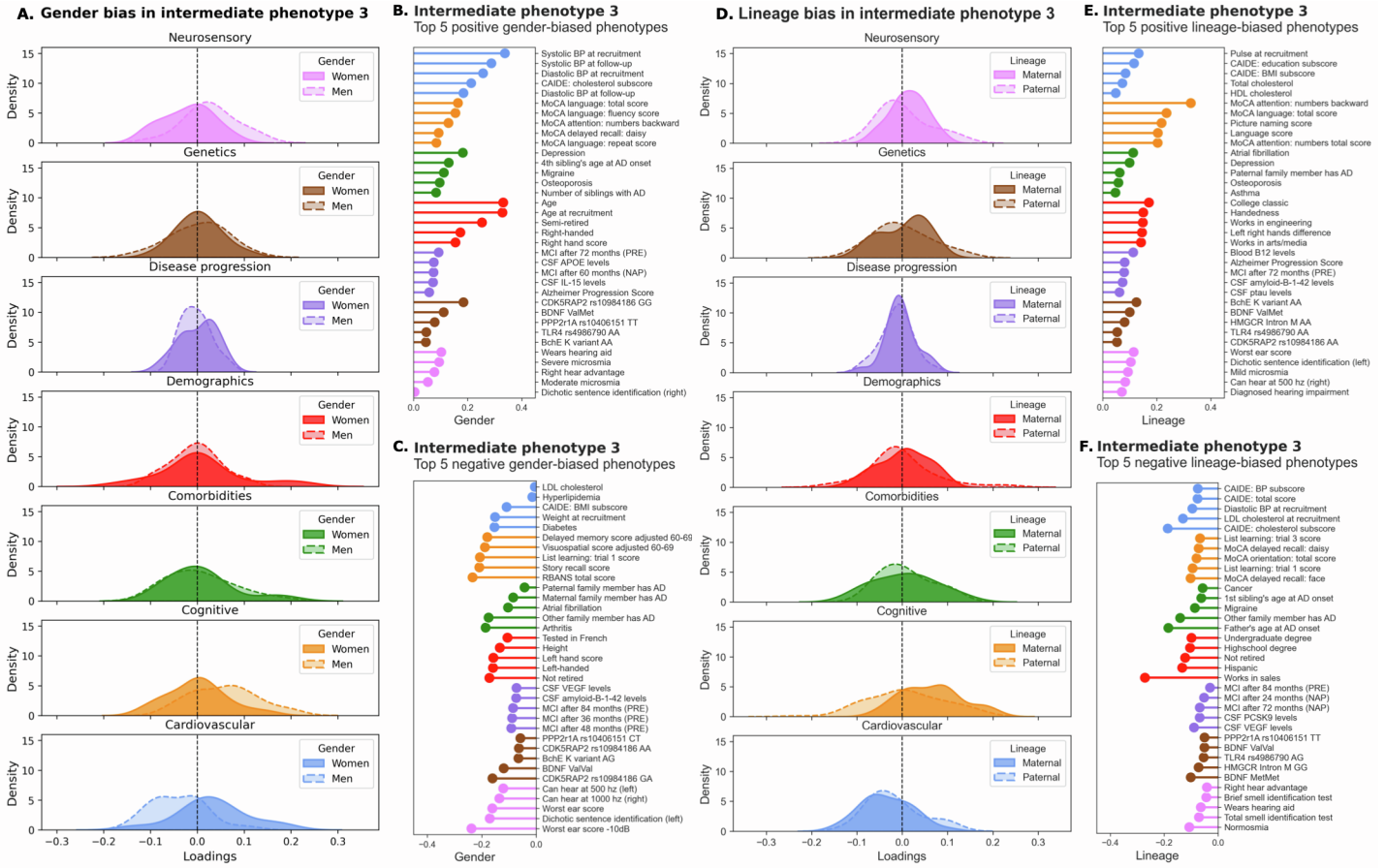

S12. Breakdown of lineage- and gender-specific biases for intermediate phenotype 3, related to Figure 4. The distribution of PLS loadings across the six categories of risk indicators is shown for the third intermediate phenotype in (A) men and women and (D) individuals with maternal and paternal AD lineage. Additional per-category breakdowns of loading differences are shown by gender in (B & C) and by AD lineage in (E & F). The third intermediate phenotype of AD susceptibility reflects a trade-off between cognitive performance and cardiovascular health, modulated by gender and parental lineage. On average, men exhibited lower cardiovascular burden alongside higher cognitive performance, whereas women showed higher cardiovascular burden and lower cognition (panel A). Cardiovascular risk factors with known gender differences, including diabetes and osteoporosis, were among the most divergent indicators between men and women (panels B & C). Overall, these findings support a trade-off between cardiovascular health and cognitive decline associated with the ε2 allele and modulated by sex-specific biological factors.

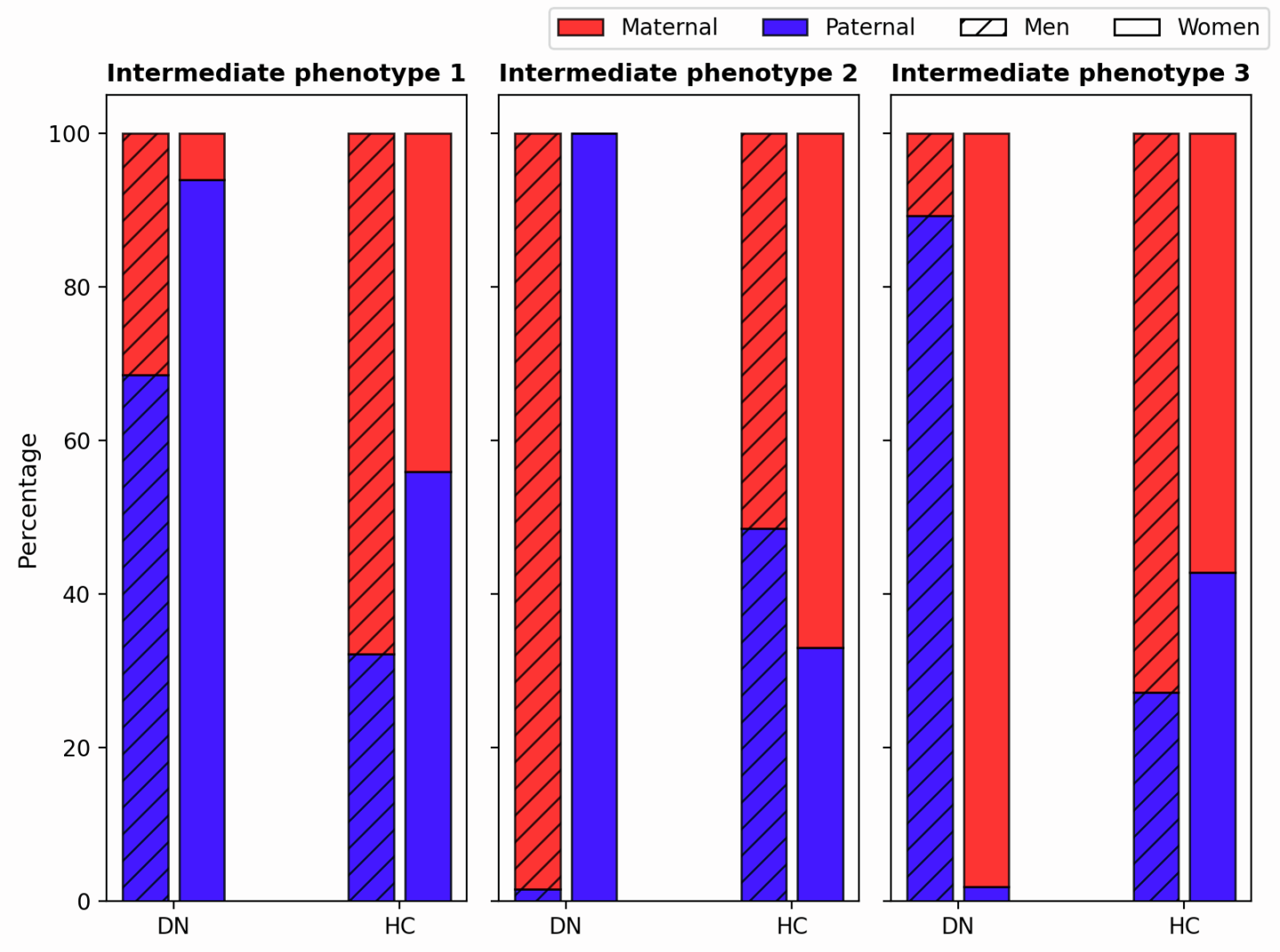

S13. Relative proportion of maternal vs. paternal effects in the default network and hippocampus of men and women probands, related to Figure 7. We present the distribution of maternal and paternal effects captured by the three intermediate phenotypes, stratified by proband gender, across the default network (DN) and hippocampus (HC). Rather than reflecting a uniform maternal–paternal contrast, each intermediate phenotype exhibits a distinct and partially dissociable lineage pattern across brain systems. For intermediate phenotype 1, paternal effects predominated over maternal effects within the default network in both men and women. In the hippocampus, maternal effects were more frequently observed, particularly in men. Intermediate phenotype 2 demonstrated a gender-dependent lineage configuration, with maternal effects spanning the default network in men and paternal effects spanning the same network in women. Conversely, intermediate phenotype 3 revealed the opposite organization, with paternal effects primarily expressed in men and maternal effects in women within the default network. Across phenotypes, the hippocampus showed a consistent predominance of maternal effects, with comparable distribution across genders. Together, these findings demonstrate that lineage effects are spatially organized and phenotype-specific rather than globally uniform, underscoring a genetically anchored and context-dependent architecture that may have been obscured in prior aggregated analyses.

	ε3/3	ε3/4	ε2/3	ε2/4	ε4/4
N (%)	195 (50.8)	123 (32.0)	42 (10.9)	16 (4.2)	8 (2.1)
Age at baseline, Mean ± SD	63.6 ± 5.2	62.3 ± 4.7	63.9 ± 6.0	64.0 ± 5.6	62.5 ± 3.0
Years of education, Mean ± SD	15.5 ± 3.5	15.2 ± 3.3	15.9 ± 3.2	15.4 ± 3.0	15.8 ± 4.1
Number of follow-up visits per person, Mean ± SD					
Women	4.1 ± 1.2	4.2 ± 1.2	4.0 ± 1.3	3.8 ± 0.8	3.7 ± 1.6
Men	4.0 ± 1.3	4.0 ± 1.1	4.1 ± 1.4	3.6 ± 1.9	5.0 ± N/A
Sex/gender (self-reported), *n* (%)					
Women	146 (74.9)	86 (70.0)	25 (60.5)	9 (56.3)	7 (87.5)
Men	49 (25.1)	37 (30.0)	17 (40.5)	7 (43.8)	1 (12.5)
Mild cognitive impairment (MCI) at 2-year follow-up, *n* (%)					
Women	4 (2.7)	3 (3.5)	0 (0.0)	0 (0.0)	0 (0.0)
Men	12 (24.5)	0 (0.0)	0 (0.0)	5 (71.4)	0 (0.0)
Mild cognitive impairment (MCI) at 4-year follow-up, *n* (%)					
Women	29 (19.9)	22 (25.5)	8 (32.0)	0 (0.0)	0 (0.0)
Men	17 (34.7)	17 (45.9)	0 (0.0)	5 (71.4)	0 (0.0)
Family history of ADRD, *n* (%)					
Women					
Maternal	101 (69.2)	61 (70.9)	18 (72.0)	9 (100.0)	7 (100.0)
Paternal	51 (34.9)	28 (32.6)	8 (32.0)	1 (11.1)	0 (0.0)
Both	6 (4.1)	3 (3.5)	1 (4.0)	1 (11.1)	0 (0.0)
Men					
Maternal	28 (57.1)	25 (67.6)	13 (76.5)	6 (85.7)	1 (100.0)
Paternal	22 (44.9)	18 (48.6)	9 (52.9)	1 (14.3)	0 (0.0)
Both	1 (2.0)	6 (16.2)	5 (29.4)	0 (0.0)	0 (0.0)

Supplementary Table S20. PREVENT-AD demographic information, related to STAR METHODS: *Human Participants*. Distribution of the demographic information from the PREVENT-AD sample grouped per *APOE* genotypes.